EPRI | ELECTRIC POWER RESEARCH INSTITUTE

Materials Reliability Program: Mitigation of PWSCC in Nickel-Base Alloys by Optimizing Hydrogen in the Primary Water (MRP-213)

1015288

Materials Reliability Program: Mitigation of PWSCC in Nickel-Base Alloys by Optimizing Hydrogen in the Primary Water (MRP-213)

1015288

Technical Update, July 2007

EPRI Project Manager

K. Ahluwalia

ELECTRIC POWER RESEARCH INSTITUTE
3420 Hillview Avenue, Palo Alto, California 94304-1338 ▪ PO Box 10412, Palo Alto, California 94303-0813 ▪ USA
800.313.3774 ▪ 650.855.2121 ▪ askepri@epri.com ▪ www.epri.com

DISCLAIMER OF WARRANTIES AND LIMITATION OF LIABILITIES

ORGANIZATION(S) THAT PREPARED THIS DOCUMENT

General Electric

Corrosion and Materials Consultancy

This is an EPRI Technical Update report. A Technical Update report is intended as an informal report of continuing research, a meeting, or a topical study. It is not a final EPRI technical report.

NOTE

For further information about EPRI, call the EPRI Customer Assistance Center at 800.313.3774 or e-mail askepri@epri.com.

CITATIONS

This document was prepared by

General Electric Global Research Center
1 Research Circle
Niskayuna, NY 12309

Principal Investigator
P.L. Andresen

Corrosion and Materials Consultancy
Baumgarten 28
D-96178 Pommersfelden
Germany

Principal Investigator
J. Hickling

This document describes research sponsored by the Electric Power Research Institute (EPRI).

This publication is a corporate document that should be cited in the literature in the following manner:

Materials Reliability Program: Mitigation of PWSCC in Nickel-Base Alloys by Optimizing Hydrogen in the Primary Water (MRP-213). EPRI, Palo Alto, CA: 2007. 1015288.

REPORT SUMMARY

The Materials Reliability Program (MRP) is investigating the effects of coolant chemistry on primary water stress corrosion crack (PWSCC) growth rates of nickel-base alloys as a possible strategy to mitigate material degradation in operating plants with components made out of Alloy 600 and its weld metals. This interim report documents the extent to which mitigation of primary water SCC growth rates can currently be expected as a result of changing the amount of hydrogen added to reactor coolant.

Background

The EPRI Primary Water Chemistry Guidelines describe the multi-faceted role of the reactor coolant in PWRs. Unfortunately, the Ni-base alloys often originally used have been found to be susceptible to PWSCC under nominal water chemistry conditions, i.e., conditions not involving impurities. In recent years, it has also become apparent that the typical level of hydrogen—25 to 35 cc/kg—added to prevent radiolysis might be unfavorable with regard to both the initiation and propagation of cracks. Optimizing hydrogen levels is thus being actively pursued as a means of mitigating component damage. Mitigating PWSCC by changes in water chemistry by such means as optimizing dissolved hydrogen levels and/or adding Zn is attractive because the potential benefit is systemic. All components are affected, and outage time is not needed for mitigating components individually. Plants also want to alter water chemistry to improve fuel utilization, avoid crud build-up on fuel, and reduce crud migration leading to high shutdown dose rates; but these efforts usually involve changes in the boron (B) and lithium (Li) levels, thus affecting the high-temperature pH (pH_T) of the reactor coolant but not the rate of cracking.

Objectives

To show that the water chemistry changes under consideration involving amount of hydrogen in reactor coolant can reduce crack growth rates (CGRs) in Alloy 600 materials. This objective is important because incipient cracking below the nondestructive evaluation (NDE) detection level may have already occurred in many Ni-base alloy components in view of the operating times already reached in many commercial plants.

Approach

The project team analyzed the most recent worldwide data on the effects of hydrogen fugacity on PWSCC and derived predictions for the expected factor of improvement from realistic changes at various operating temperatures. Because previous investigations have sometimes been less than satisfactory, mainly because of the extensive scatter observed in absolute CGRs even under nominally identical test conditions, the project team used a novel testing program involving step changes in water chemistry on-line and real-time observation of the response in crack propagation behavior of instrumented, precracked Alloy 600 specimens exposed at constant stress intensity in high-temperature autoclaves.

Results

There is a reasonable theoretical basis, supported in particular by extensive test data from the naval reactors program, to recommend moving to higher H_2 levels in PWR primary water to obtain some mitigation of PWSCC for nickel-base alloys used in thick-wall components. Such a change is expected to always have a positive effect in slowing down crack growth, independent of the material or operating temperature. Quantifying the predicted benefit of such a change for any particular component is complex because it depends on the material, the temperature, the starting H_2, the new H_2 target, and other factors. Overall, the absolute benefit of H_2 optimization will be greater at higher temperatures such as those that occur in the pressurizer and for higher-strength alloys. For just over two years, the MRP has sponsored a test program that, while limited in scope compared to the literature data, attempts to confirm the theoretical predictions of CGR. The focus to date has been on increasing H_2 fugacity in steps up to a maximum value of 80 cc/kg. In almost all cases studied, there has been a short-term decrease in the measured CGR that exceeds the expected response. Over longer periods of time, the CGRs sometimes rise again; and there is some scatter in the observations from specimen-to-specimen and test-to-test.

EPRI Perspective

Because the influence of H_2 fugacity on PWSCC has been observed for both initiation and growth in nickel-base alloys by many laboratories throughout the world in tests involving hundreds of data points, there is ample basis for confidence that the effect is real. The data presently available from the MRP test program support the beneficial effects of increasing H_2, but the use to date of Alloy 600 where the predicted benefits of the chosen step changes in H_2 are lower than for weld metals and specimen-to-specimen variations make the interim results less clear than desired. Testing will continue throughout 2007 and into 2008, focusing primarily on Alloy 182; and a full analysis of the data will be available in the second half of 2008. A small effort will be also be made to examine possible synergistic effects of adding Zn together with increasing H_2.

Keywords

Pressurized water reactor
Primary water chemistry
Alloy 600
Primary water stress corrosion cracking
Mitigation of cracking
Crack growth rate

CONTENTS

LIST OF FIGURES

LIST OF TABLES

1 INTRODUCTION

This report is designed to summarize the current MRP position regarding possible mitigation of stress corrosion cracking (SCC) of nickel-base alloys in PWR primary water (PWSCC) by optimizing the H_2 fugacity. Mitigating SCC by changes in water chemistry is attractive, because benefits are potentially systemic – i.e., all wetted components are affected, and outage time is not used by mitigating components individually. Two main chemistry mitigation approaches are being considered by the MRP (either separately or together), namely optimizing H_2 fugacity and adding Zn, but only optimized H_2 is considered here. Both increased and decreased H_2 fugacity can theoretically provide benefits and may be feasible, but radiolysis – leading to increased corrosion potential and thus elevated crack growth rates (CGRs) – is a serious concern at sufficiently low H_2. Changes in the B/Li chemistry (and associated high temperature pH) have little effect on SCC growth [1, 2], consistent with the fact that in deaerated water, the corrosion potential is controlled by the H_2/H_2O reaction (Figure 1-1), and the H_2/H_2O line is exactly parallel to the metal-metal oxide phase boundaries.

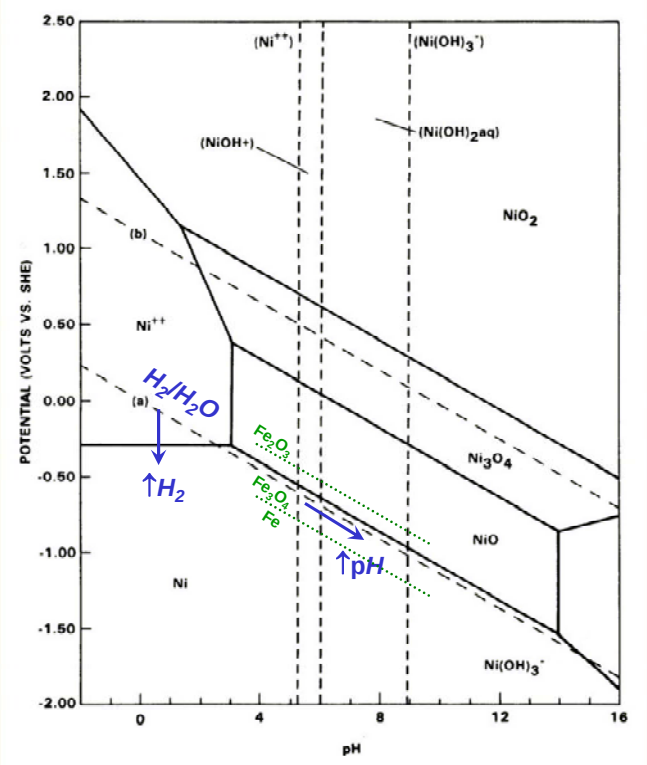

Figure 1-1
Pourbaix (potential – pH) Diagram for the High-Temperature Ni-H_2O System, Showing the Close Proximity of the H_2 / H_2O Line (shown for 1 atm. H_2) with the Ni / NiO Line.

Note:
The H_2/H_2O line controls the corrosion potential in de-aerated water and is parallel to the Ni/NiO (and Fe/Fe_3O_4 and Cr/Cr_2O_3) lines, so changes in pH do not change the proximity of the corrosion potential to the metal-oxide phase boundaries. However, changes in H_2 can cause the corrosion potential to traverse the Ni/NiO phase boundary, and this is much more likely to affect SCC response.

It is helpful to understand and put in context (Figure 1-2) the effects of potential associated with changes in H_2 vs. O_2 (or other oxidants). The presence of oxidants in the bulk water causes the corrosion potential of the free surface to be markedly elevated, often by 500 – 700 mV. Because O_2 is consumed as it diffuses into the crack, there is a gradient in O_2 and therefore a gradient in potential within the crack. This gradient concentrates anions into the crack (and decreases the non-H^+ cation concentration). The resulting change in crack chemistry usually has a large effect on crack growth rate.

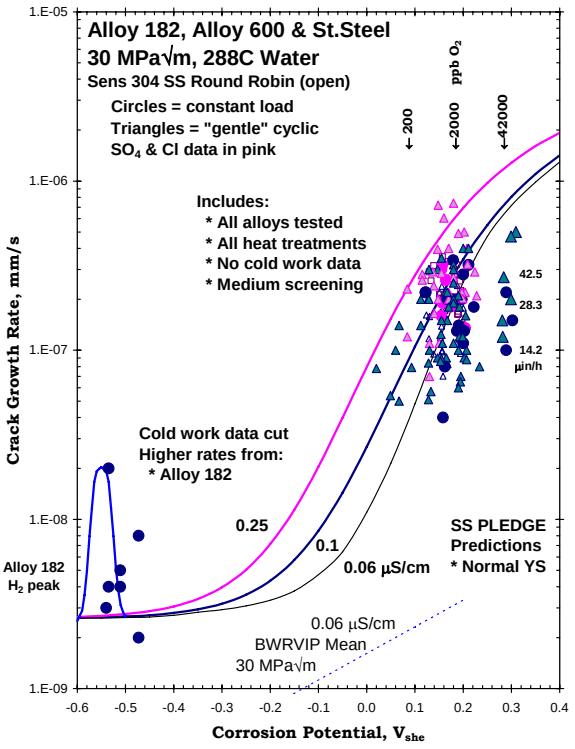

Figure 1-2
Crack Growth Rate of Ni Alloys in High-Temperature Water as a Function of Corrosion Potential

Note:
In deaerated water, Ni alloys exhibit a small peak in growth rate at the Ni/NiO phase boundary as a function of H_2 (i.e., near -550 mV_{she} in pure water) [20].

By comparison, the presence of H_2 in the bulk water has a much smaller effect on corrosion potential (59.3 mV per 10X change in H_2 at 325°C). There is no consumption of H_2 within the crack (there may be some creation of H_2 from corrosion reactions), so there is essentially no potential gradient, and any effect of H_2 fugacity is associated only with a small shift in the corrosion potential (both at the free surface and at the tip of an existing crack). For iron-base alloys, such as stainless steels, these small changes do not significantly affect CGRs. With nickel-base alloys, however, they can result in an important change in the composition and stability of the passive films as a result of crossing the Ni/NiO phase boundary (Figure 1-1). The magnitude of the expected changes in potential and crack growth rate associated with changes in H_2 in pure water is shown schematically in Figure 1-2 by the small peak around the corrosion potential (i.e., near –550 mV_{she}). Agreement with the measured CGR data for Alloy 182 is not exact, however, and is strongly influenced by loading and material factors (e.g., cold work and yield strength).

Focusing on the effect of H_2 in *deaerated* water, Figure 1-3 presents a schematic of the CGR vs. H_2, and shows peaks for materials like Alloy 600 that exhibit a ~3X peak and for materials like Alloy 82 weld metal that exhibit a ~8X peak (a more detailed description of the CGR peak is provided in Section 2.3). The relationship between H_2 and corrosion potential (ECP) is shown on

the top scale, although the specific potential will depend on the solution pH_T (which shifts the corrosion potential by 118.6 mV/pH at 325°C) and the scaling vs. H_2 depends to a limited extent on temperature (59.3 mV per 10X change in H_2 at 325°C, and 55.9 mV at 290°C). Figure 1-3 emphasizes the limited change in CGR expected if the change in H_2 is limited, e.g., to 2X. While the CGR peak might be 8X, a 2X increase in H_2 from the peak value would only decrease the CGR by 1.34X.

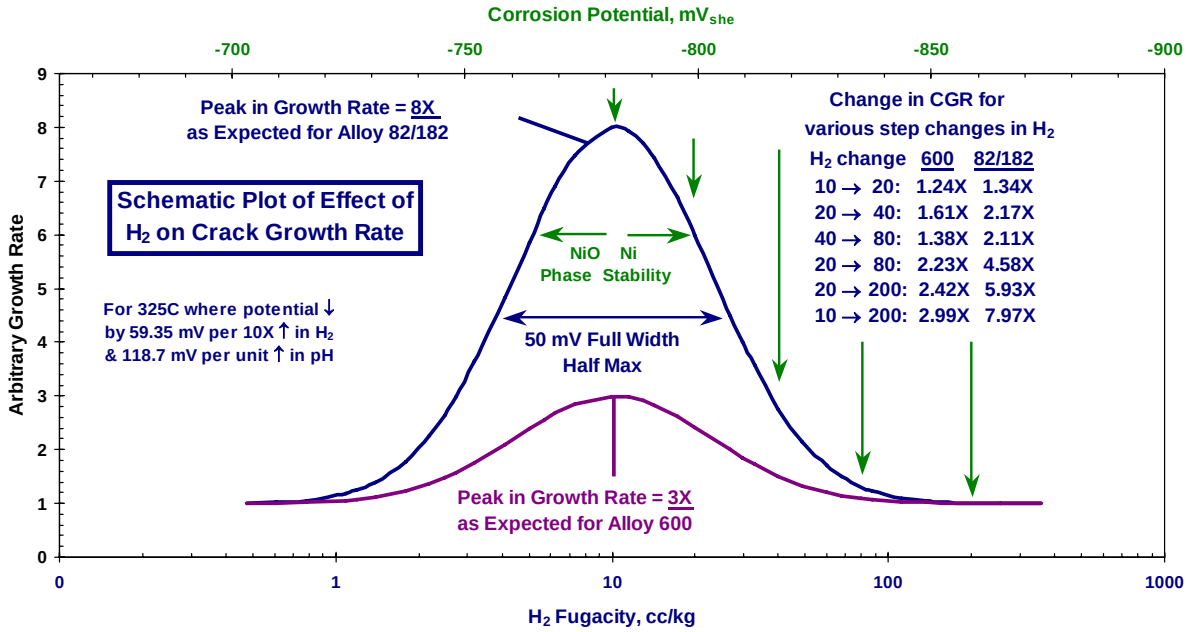

Figure 1-3
Previous MRP Schematic of Expected H_2 Effects on PWSCC Growth Rate at 325°C

Note:
All nickel-base alloys appear to show a peak in crack growth rate close to the H_2 fugacity associated with the Ni/NiO phase boundary. The primary difference among them is thought to be the height of the peak, which varies from 2.5 – 3X for alloy 600 to 5 – 8 for alloy 182/82 weld metals and alloy X750 (and probably other higher yield strength Ni alloys) [1, 2].

The location of the Ni/NiO phase boundary as a function of H_2 depends strongly on temperature (Figure 1-4 and Figure 1-5). Based on available thermodynamic data, the location of the phase boundary was once thought to occur at higher H_2 (upper curves in Figure 1-4) compared to the more recent and detailed studies by Attanasio and Morton [3] (lowest curves in Figure 1-4). Attanasio and Morton used contact electrical resistance (CER) measurements and direct observation of the surface appearance of coupons to establish the location of the Ni/NiO phase boundary. They also analyzed their extensive CGR data and formulated a model to describe the CGR in the vicinity of the Ni/NiO phase boundary; this model has been modified here to make it more flexible, as discussed in Section 2.3.

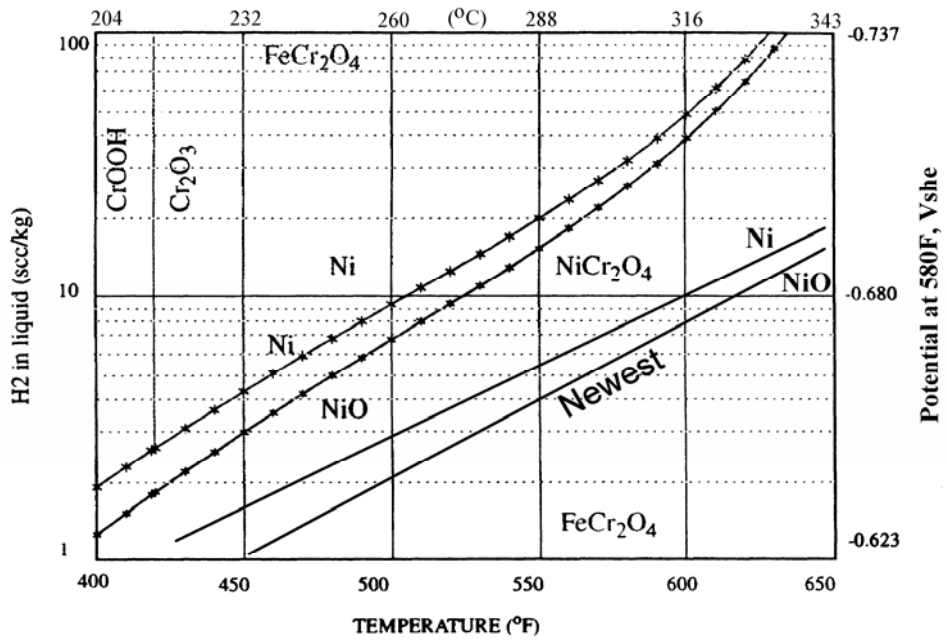

Figure 1-4
Dependence of the Ni/NiO Phase Boundary on Temperature and Dissolved H_2

Note:
The lower curve represents modern data and calculations [1, 2, 3, 11].

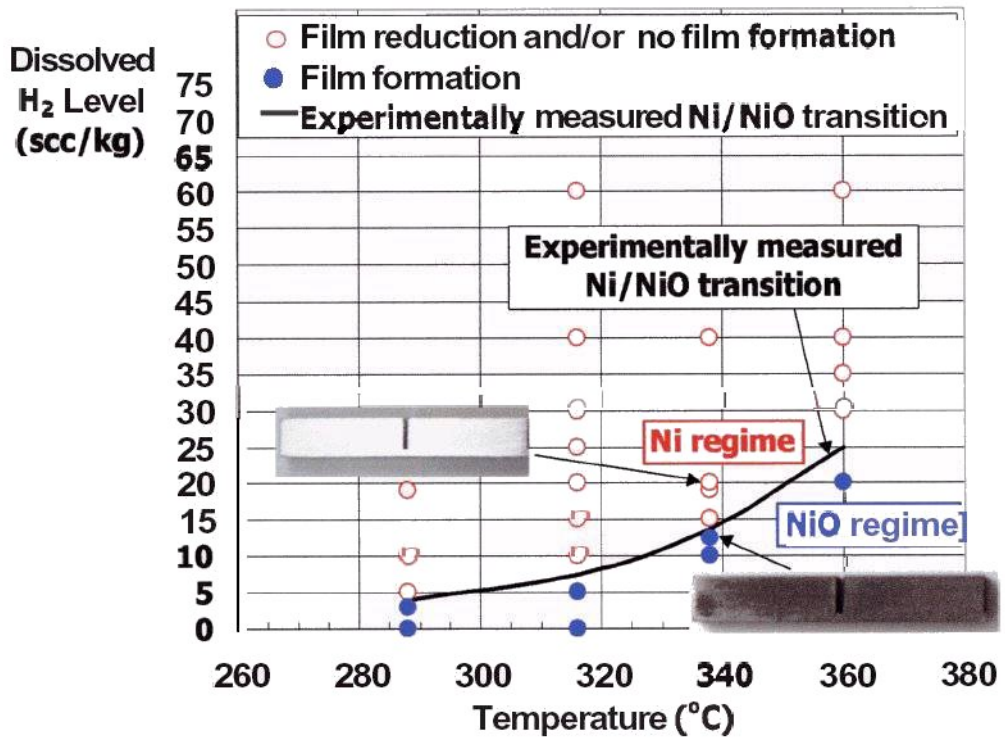

Figure 1-5
Experimental Observations [3] of the Dependence of the Ni/NiO Phase Boundary on Temperature and Dissolved H_2 using Coupons and the CER Technique.

2
DETAILED EFFECTS OF H_2 FUGACITY ON SCC OF NICKEL-BASE ALLOYS

While the mechanistic origin is unclear [4, 5], there are many, consistent data from a number of laboratories showing that SCC initiation and growth rates (CGR) of nickel-base alloys exhibit a peak near the Ni/NiO phase boundary [3, 6]. The effects of H_2 on initiation and growth are considered separately in the next two sections, but – for thick-section materials – more weight should be given to the CGR data, since it has to be assumed that incipient cracks (below the NDE detection limits) have already initiated in many components in service and therefore propagation usually represents the most pressing problem. Nonetheless, new crack initiation will continue to occur with increased time of plant operation, and mitigating initiation is thus also important to manage SCC over the long term.

2.1 Defining the Ni/NiO Phase Boundary

There are two primary issues in determining the Ni/NiO phase boundary for practical use in high temperature water: the thermodynamics of the Ni/NiO phase boundary, expressed in terms of the fugacity of H_2 (f_{H2}) at temperature, and the H_2 fugacity *coefficient* vs. temperature that provides a way to convert to room temperature H_2 concentration, e.g., in cc/kg or ppm. A simplified approach that directly expresses the Ni/NiO phase boundary in terms of room temperature H_2 is provided as a more useful engineering tool (see Equation 2-2).

The Ni/NiO phase boundary and associated Ni-spinel phase boundaries were once estimated (based on available thermodynamic data) as shown in Figure 1-4 (top two curves). Morton and co-authors subsequently performed a variety of measurements that showed that these calculated phase boundary locations were in error, and they published two somewhat different formulations [3, 6]. Morton [7] has indicated that the more definitive one is as expressed in reference [3], which also shows the underlying contact electrical resistance (CER) and coupon data (Figure 1-5). The formulation for H_2 fugacity (f_{H2}) *at temperature* in that paper is:

$$\ln(f_{H2}) = -4619.2 / T(K) + 5.2302 \qquad \textbf{Eq. 2-1}$$

This is represented by lowest curve in Figure 1-4, which expresses the result in terms of room temperature H_2 in cc H_2 per kg H_2O (cc/kg). The room temperature H_2 level that corresponds to the Ni/NiO phase boundary is of greater practical use to experimentalists and plant operators than the high-temperature H_2 fugacity. Neither the CER/coupon data nor the H_2 fugacity coefficient data are precise enough to merit fitting to anything more complex than a simple power law (linear when plotting log(H_2) vs. temperature). The fit chosen here is:

$$\text{cc/kg } H_2 \text{ at Ni/NiO Boundary} = 10^{(0.0111*T(°C) - 2.59)} \qquad \textbf{Eq. 2-2}$$

To convert between H_2 fugacity at temperature and H_2 concentration (cc/kg or ppm) at room temperature requires knowledge of the H_2 fugacity coefficient. If water with a fixed concentration of H_2 is heated, the H_2 fugacity varies, decreasing to ~20% of its room temperature value at 289°C and to ~10% at 335°C. A key historical reference is the work by Fernandez-Prini and coworkers [8] (Figure 2-1). Unpublished work by Moshier and Witt is referenced by Attanasio and Morton [3], with these data listed in Table 2-4 of [3] as the "Henry's Law Coefficient" – note that the units are not directly fugacity coefficient, but rather atm/(cc/kg). Since 1 atm of H_2 bubbled in 25°C water gives 1.58 ppm or 17.7 cc/kg, at 25°C the table value would be 1/17.7 = 0.0565. Their value at 288°C is 0.0122 and the corresponding H_2 fugacity coefficient is 0.0122 x 17.7 = 0.216.

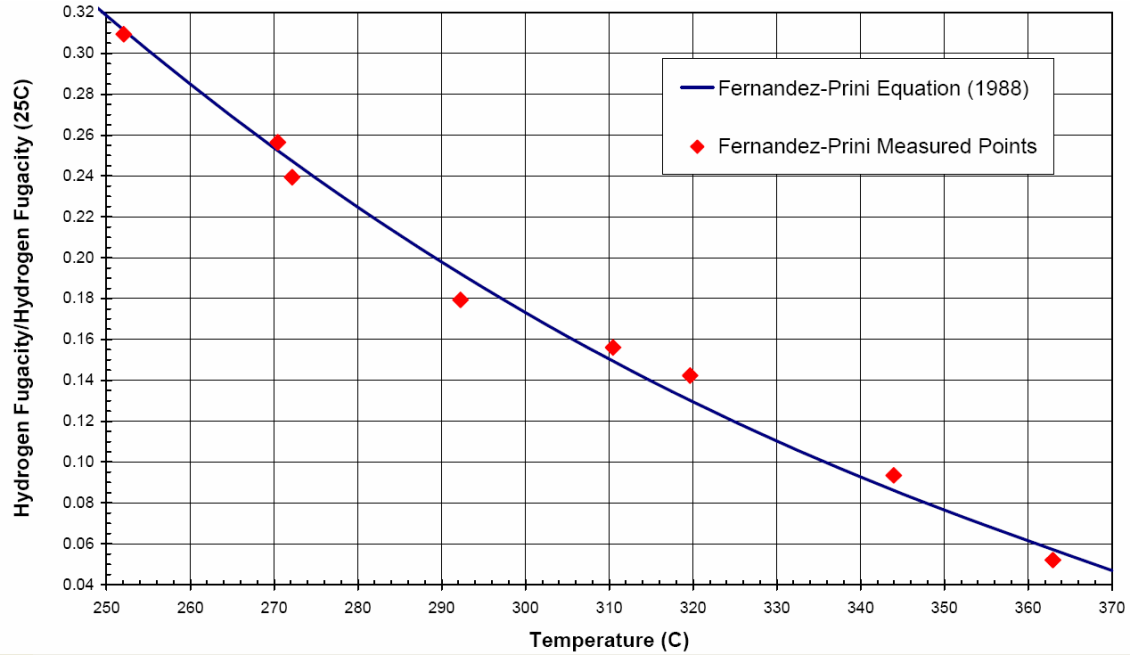

Figure 2-1
H_2 Fugacity Coefficient vs. Temperature, Showing That 1 Bar H_2 at 25°C Yields only 0.12 Bar H_2 at 325°C [8]

If one compiles a list of H_2 fugacity coefficients vs. temperature from the Moshier and Witt data (Table 2-1 and Figure 2-2), it shows good agreement with the Fernandez-Prini data at lower temperatures, then deviates in a somewhat peculiar fashion with increasing temperature – i.e., it appears as if there is a sudden offset between 300 – 315°C. It is possible to draw a straight line that fits the Moshier and Witt data reasonably well, but this leaves open the question of why there is a difference with the Fernandez-Prini data, and why the Moshier and Witt data are linear vs. temperature and the Fernandez-Prini data are not. Possible issues include differences in technique (Moshier and Witt used an at-temperature Ag-Pd membrane and pressure gage), differences in system over-pressure (this is not enough to account for the discrepancy, but is not negligible – Fernandez-Prini apparently used saturation pressure), and possibly different water chemistry and pH (Attanasio and Morton, and presumably Moshier and Witt, used a pH additive that gave a $pH_T = 7$).

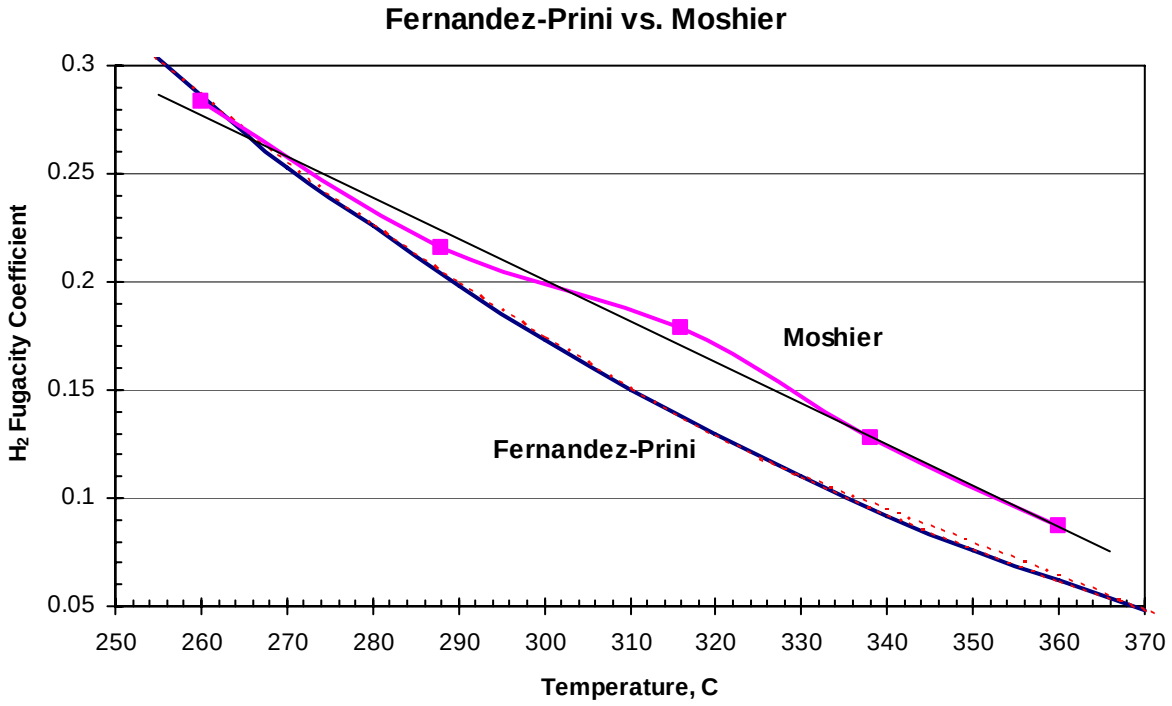

Figure 2-2
H_2 Fugacity Coefficient vs. Temperature, Showing That 1 Bar H_2 at 25°C Yields only 0.12 Bar H_2 at 325°C [8]

Table 2-1
The Ni/NiO Phase Boundary and H_2 Fugacity Coefficients vs. Temperature

Parameter	Temperature, °C						
	250	270	290	310	325	340	360
Ni/NiO Boundary in cc H_2 / kg H_2O[1]	1.5	2.6	4.2	7.1	10.4	15.3	25.5
H_2 Fugacity Coeff. Moshier & Witt Fit	0.30	0.26	0.22	0.18	0.15	0.13	0.087
H_2 Fugacity Coeff. Fernandez-Prini Fit	0.32	0.25	0.20	0.15	0.12	0.091	0.062

[1]The Ni/NiO phase boundary can be calculated: $10^{(0.0111*T(°C) - 2.59)}$ cc/kg H_2

Whatever the origin of the difference in H_2 fugacity coefficient, the actual observations by Attanasio and Morton using CER and coupon data can be directly used (Equation 2-2 and Figure 1-5): a known H_2 gas concentration was equilibrated in room temperature water, then heated and used for both CER measurements and coupon exposure observations. Thus, the relationship shown in Figure 1-5 (and the lowest curve in Figure 1-4) and expressed in Equation 2-2 are accurate within the limits of their data. The CGR peak in the vicinity of the Ni/NiO phase boundary is described further in Section 2.3.

2.2 Expected Influence of H_2 Fugacity on PWSCC Initiation in Nickel-Base Alloys

Starting in 1996, EPRI attempted to correlate and model the diverse results reported over many years on the effects of H_2 fugacity on PWSCC initiation in Alloy 600. These efforts culminated in 2005 in the dependency shown in Figure 2-3. The relevant MRP-147 report [9] also contains a comparison of the initiation model for H_2 dependency with CGR data obtained by Morton et al. [6], which is discussed in more detail in the next section. As shown in Figure 2-4, the agreement is very good and provides strong support for the concept that PWSCC behavior is determined by the proximity of the corrosion potential to the Ni/NiO phase boundary. New laboratory data on crack initiation for Alloy 600, released in 2005 [10] and shown in Figure 2-5, also confirm the similarity in SCC behavior of nickel-base alloys for both crack initiation and crack growth as a function of H_2 level. There appears to be little or no data on the H_2 effect for crack initiation in other nickel-base alloys, but it is reasonable to speculate that the effect of varying H_2 might be stronger on Alloy 182/82 weld metal, Alloy X-750, etc. as has been observed for crack growth.

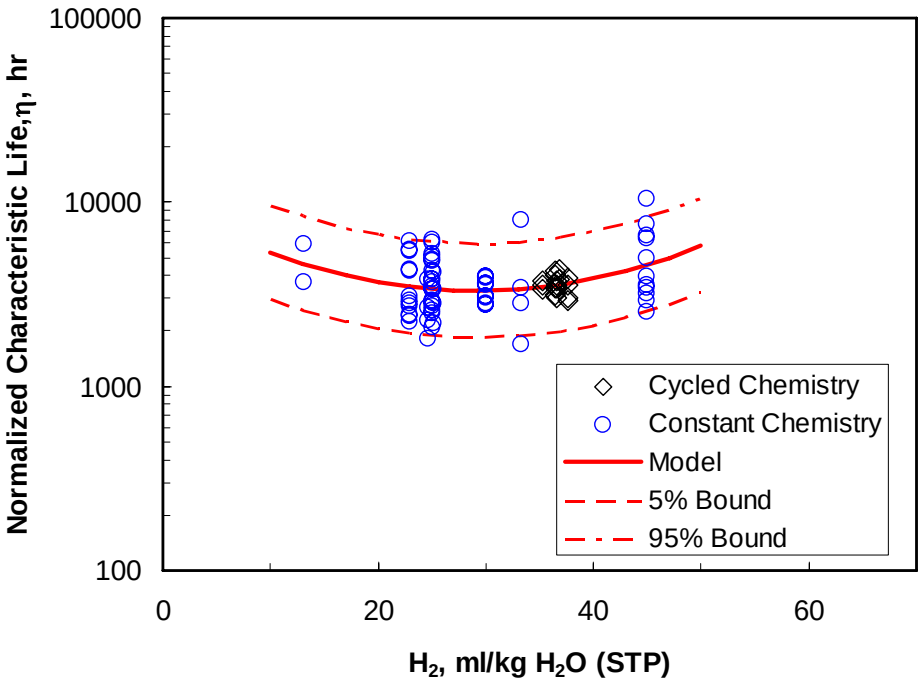

Figure 2-3
Conclusion from MRP-147 Regarding Dependency of PWSCC Initiation Behavior on H_2 Fugacity at 330°C (considered valid over a temperature range of ±10°C) [9]

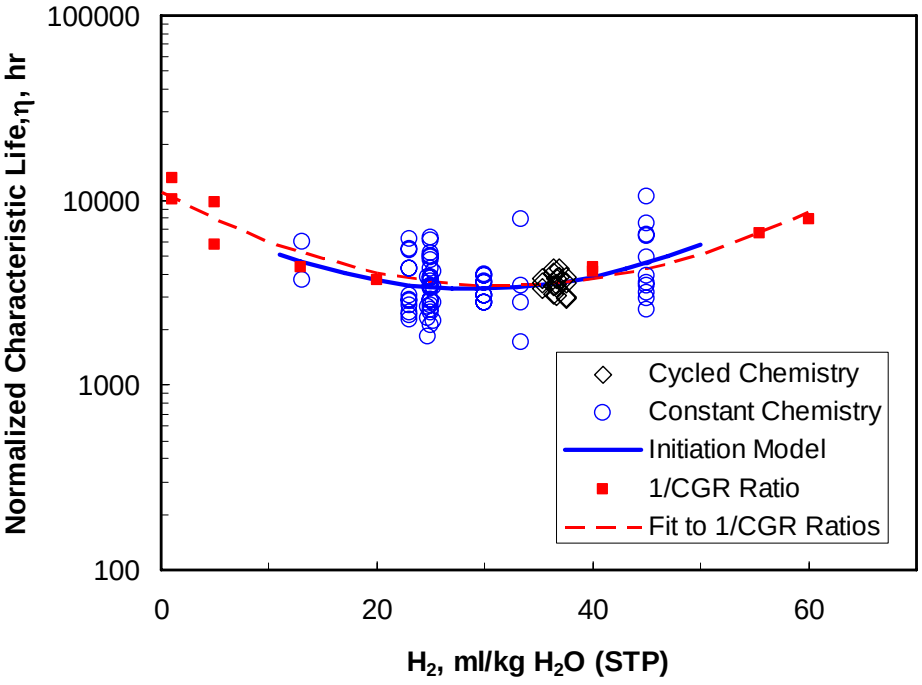

Figure 2-4
Comparison of Initiation Model H_2 Term and Data at 330°C with Scaled Inverse Ratios of Crack Growth Rate from Morton, et al [6] at 338°C on Alloy 600 [9]

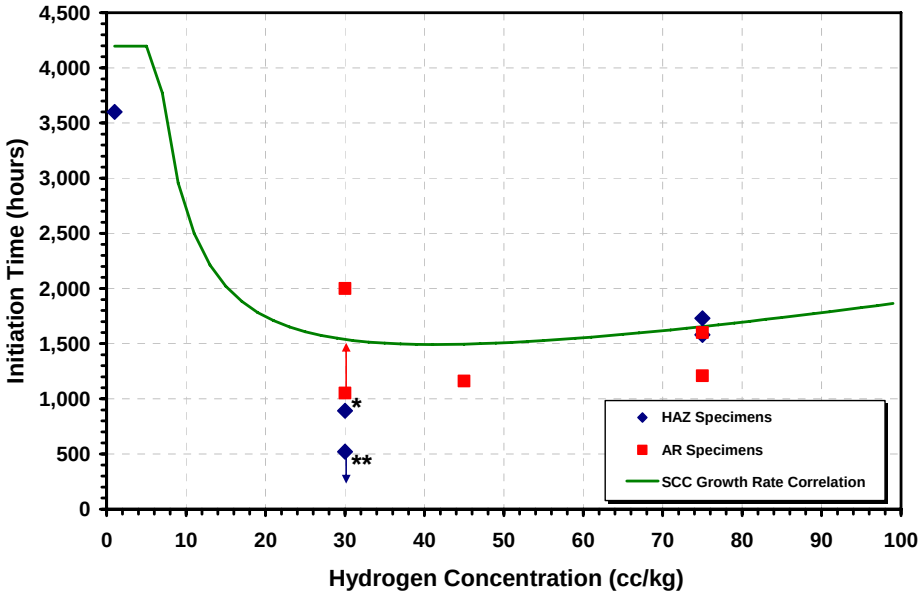

* Two small cracks observed after tensile pull, not detected by EPD (time represents exposure time)
** Multiple cracks observed prior to tensile pull, not detected by EPD (time represents exposure time)

Figure 2-5
Recent Laboratory Data of Richey, et al [10] on SCC Initiation of Alloy 600 as a Function of H_2 Concentration

2.3 Effect of H_2 Fugacity on PWSCC CGRs in Nickel-Base Alloys

The most extensive work in this area has been performed by Morton et al. at the Lockheed-Martin KAPL laboratories within the naval reactor test program [3, 6—7, 11, 12]. Figures 2-6 – 2-11 show that this phenomenon spans all nickel-base alloys that have been studied, including Alloy 600 (both base metal and HAZ), Alloy 182/82 weld metals, Alloy X-750, etc. It is important to realize, however, that water chemistry effects are often a secondary factor in the PWSCC growth rate of nickel-base alloys when compared with the influence of stress intensity factor (K) or material condition (e.g., heat, heat treatment, and cold work). This is illustrated, e.g., for Alloy 82 in Figure 2-12, taken from recently published work by Paraventi and Moshier of the Bettis laboratories [13]. However, both temperature and H_2 have *relative* effects (ratio of two growth rates) that appear to be weakly dependent on such factors as K or material condition – that is, the effects of temperature and H_2 are always present and essentially unchanged independent of other factors. Therefore, a factor-of-improvement (FOI) analysis should provide a reasonable *estimate* of the expected benefit to be obtained from a change in H_2.

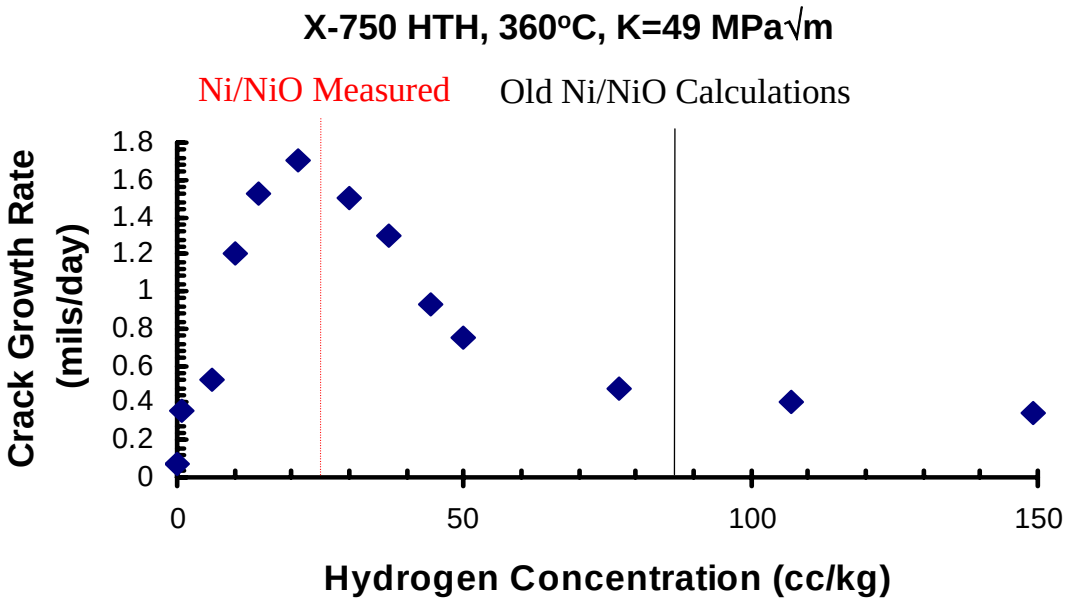

Figure 2-6
Crack Growth Rate of Alloys X750 HTH in High-Temperature Water as a Function of H_2 Concentration (17.7 cc/kg = 1.6 ppm = 1 atm H2 bubbled into pure water at 25°C) [6]

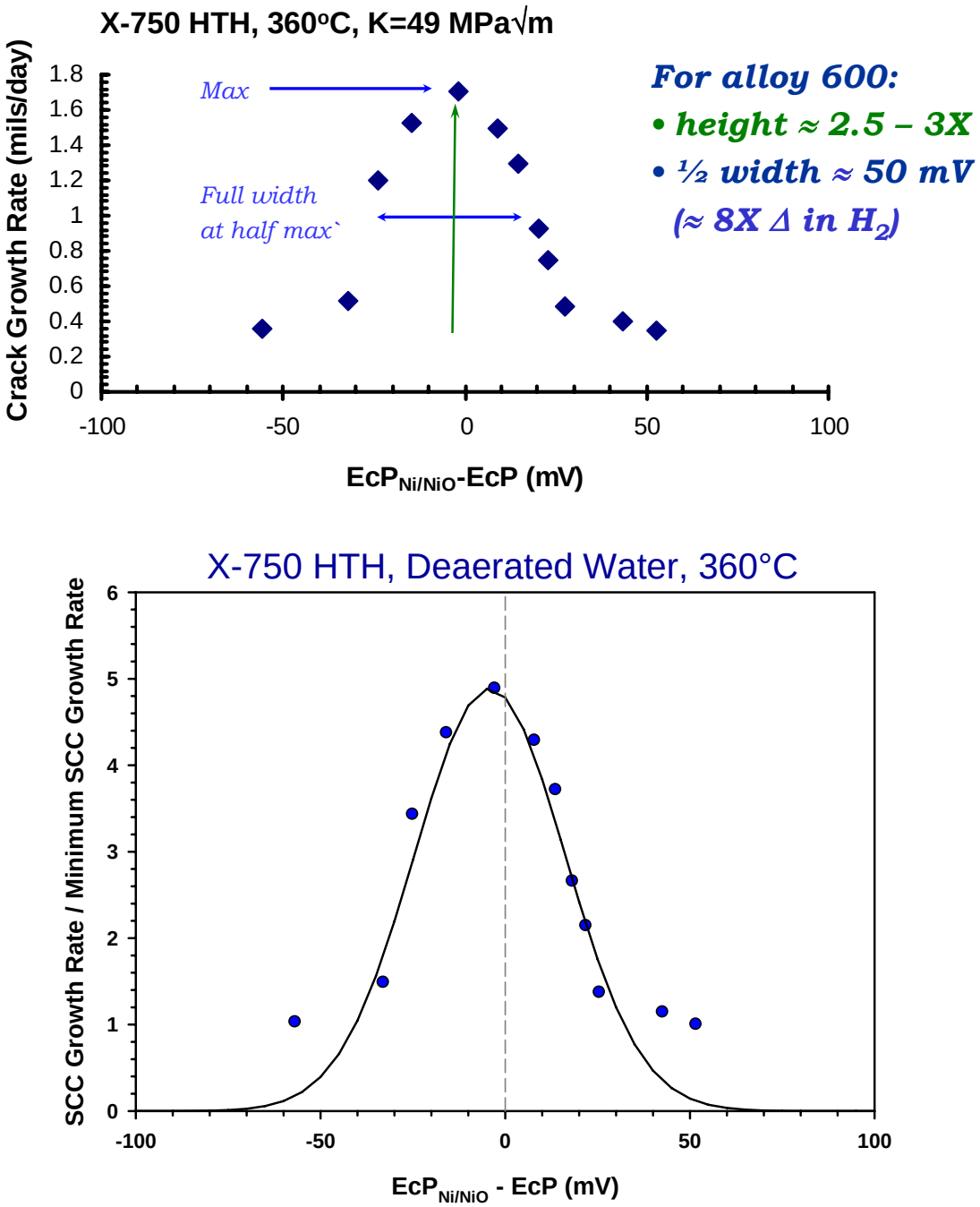

Figure 2-7
Crack Growth Rate of Alloy X750 HTH in High-Temperature Water as a Function of Potential Rather than H_2 (see Figure 2-6)

Note:
The peak growth rate occurs very close to the Ni/NiO phase boundary, with a characteristic height and width associated with the material and condition [6].

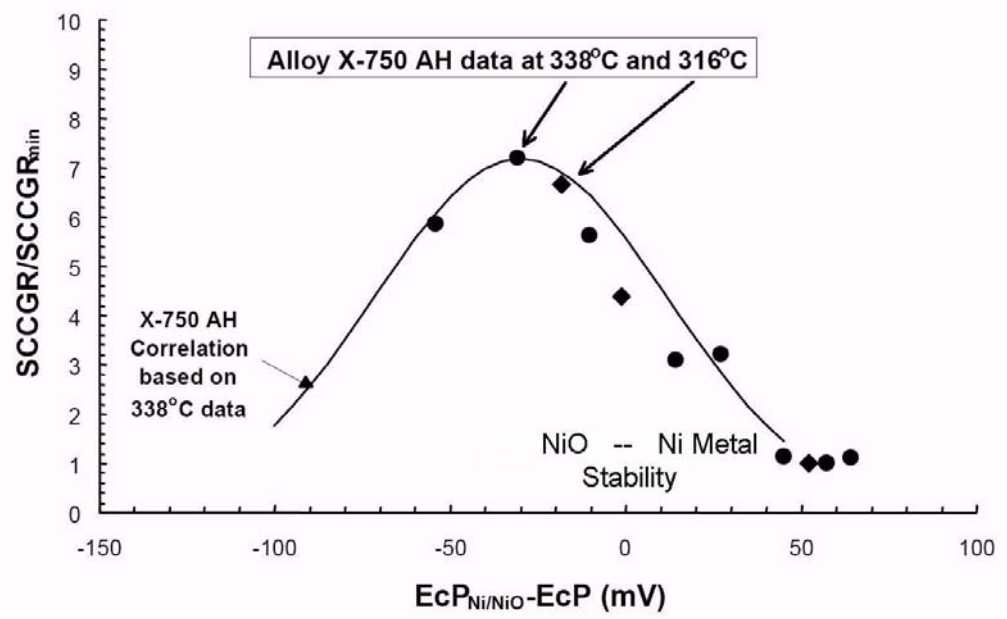

Figure 2-8
Crack Growth Rate of Alloys X750 AH in High-Temperature Water as a Function of Potential Rather than H_2

Note:
For this particular heat treatment (AH) the peak growth rate appears to occur at a moderate *offset* from the Ni/NiO phase boundary, with a characteristic height and width associated with the material and condition [6].

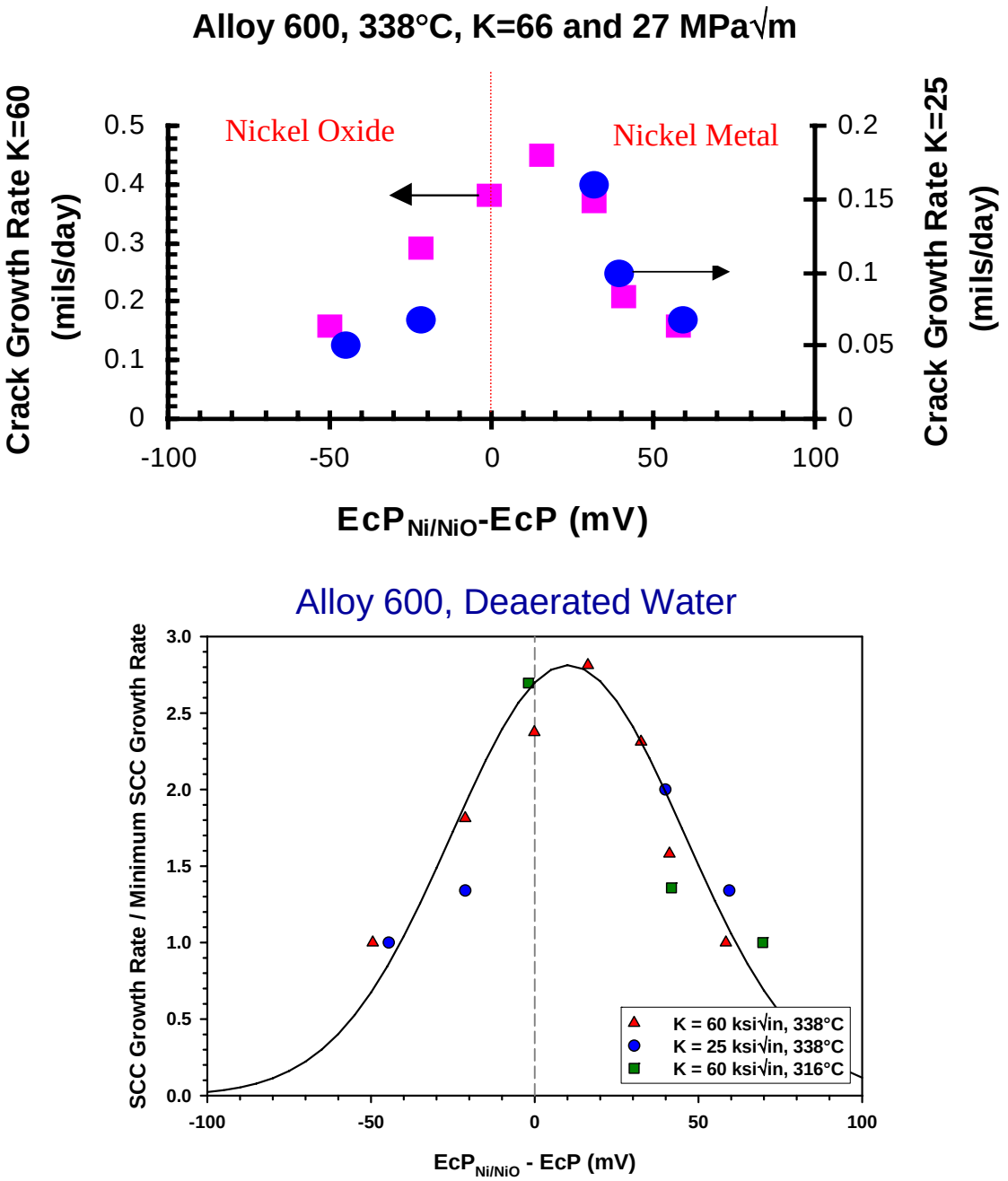

Figure 2-9
Crack Growth Rate of Alloy 600 in High-Temperature Water as a Function of Potential/H_2

Note:
The peak growth rate occurs very close to the Ni/NiO phase boundary, with a characteristic height and width associated with the material and condition [6].

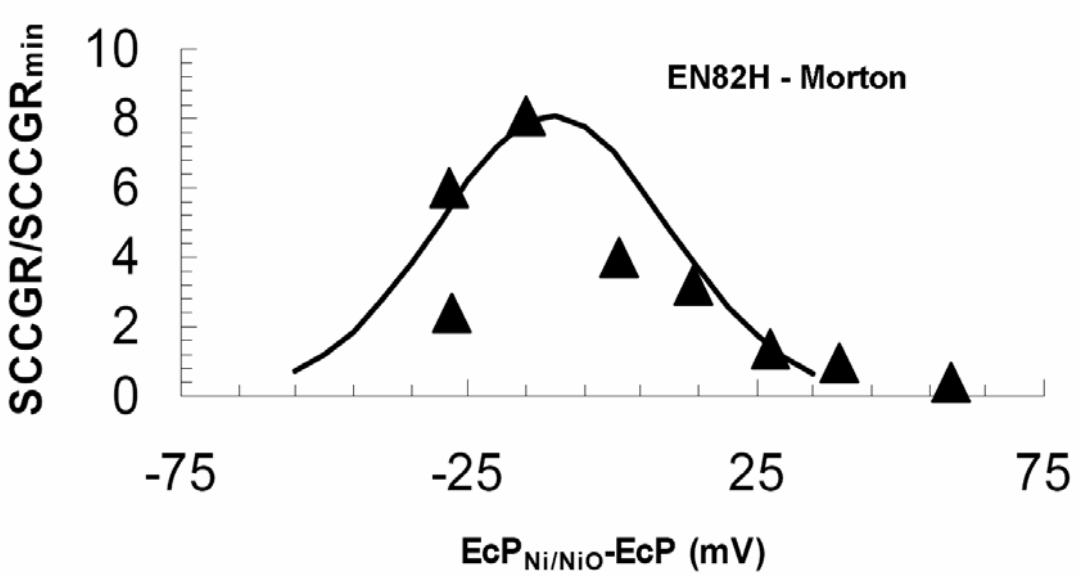

Figure 2-10
Crack Growth Rate of Alloy EN82H Weld Metal in High-Temperature Water as a Function of Potential

Note:
The peak growth rate occurs close to the Ni/NiO phase boundary, although it may be 5—10 mV into the NiO stability regime (i.e., at lower H_2 than the Ni/NiO transition) [3].

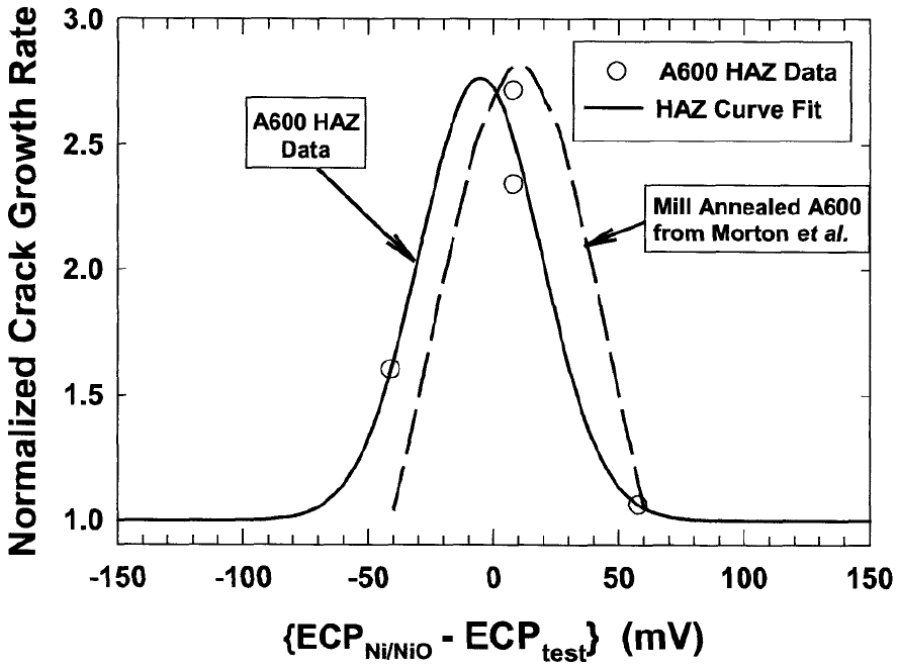

Figure 2-11
Comparison of the Effect of Electrochemical Potential on the Crack Growth Rate of Alloy 600 Base Material and on the Alloy 600 Heat Affected Zone [12]

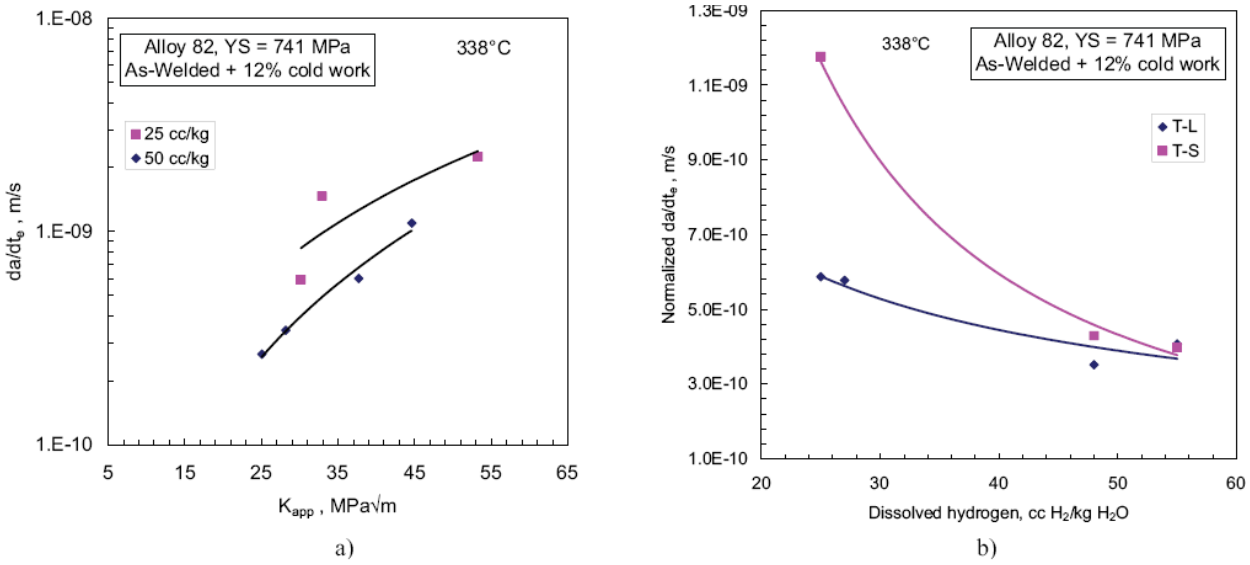

Figure 2-12
Comparison of SCC Rates Measured on Cold-Rolled Alloy 82 as a Function of Applied K at 25 and 50 cc H_2/kg H_2O at 338°C (a) and SCC Rates Normalized to 30 MPa√m and Plotted Separately as a Function of Weld Specimen Orientation (b)

Note:
The increase in growth rate at lower dissolved H_2 levels is greater in the T-S than in the T-L orientation [7].

Because the effect of H_2 on SCC has been observed for both initiation and growth of nickel-base alloys, and by many laboratories throughout the world involving hundreds of data points, there is ample basis for confidence that the effect is real. Additionally, the corrosion potential of nickel-base alloys (and other high Cr materials) responds very thermodynamically to changes in H_2 fugacity. Andresen et al. [1, 2] and Attanasio and Morton [3, 11] showed that above some low H_2 level (which is « 1 cc/kg in pure water or B/Li solutions, but ~ 5 cc/kg in the buffered environment (not B/Li) used in the KAPL tests), high alloy materials exhibit corrosion potentials (ECP) very close to that observed on Pt (Figures 2-13 and 2-14). Indeed, in pure water, thermodynamic ECP response is observed at least down to 10 ppb H_2 (~0.1 cc/kg H_2). Thus, these materials respond quickly and reproducibly to changes in H_2 level.

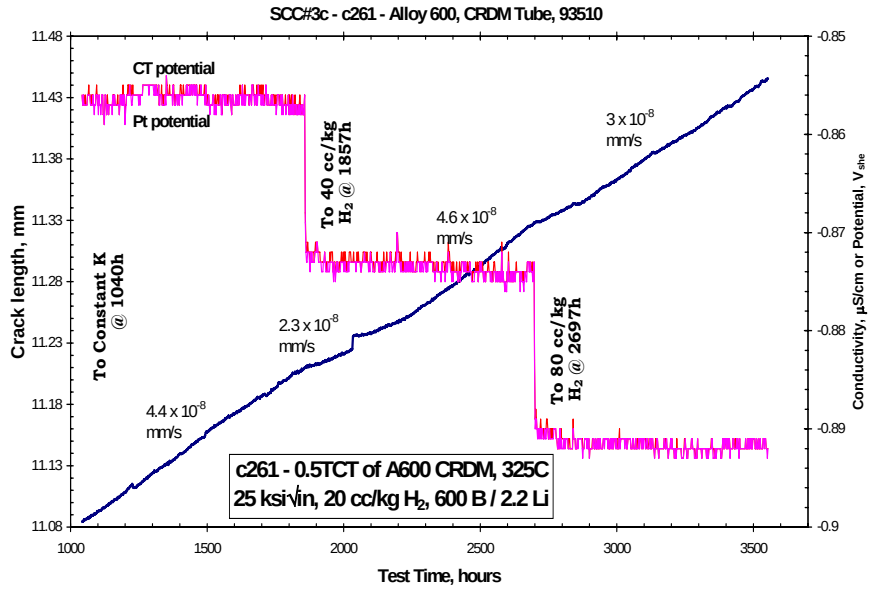

Figure 2-13
Effect of H_2 Step Changes on SCC Growth Rate of Alloy 600 and on the Corrosion Potential of Pt and Alloy 600

Note:
Because the peak height for the effect of H_2 on Alloy 600 is only 2.5—3X, for limited changes in H2 (e.g., the 2X changes shown in Figure 2-13), only a limited – and sometimes transient – reduction in SCC growth rate is observed [1, 2].

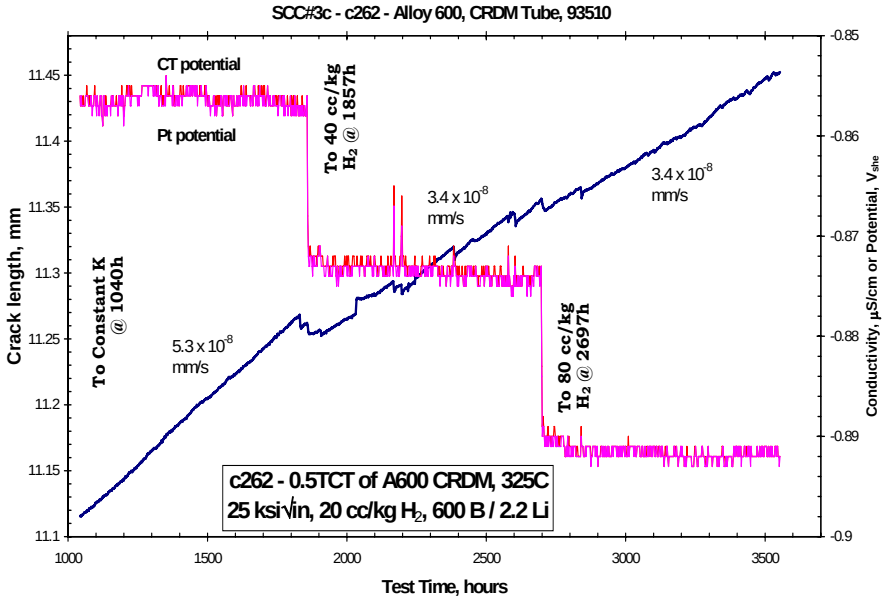

Figure 2-14
Corresponding Data to Figure 2-13 Obtained from a Duplicate Specimen in the Same Autoclave

Attanasio and Morton et al. [3] modeled the CGR peak near the Ni/NiO phase boundary, expressing it in terms of a relative growth rate, where a value of 1 is the CGR at very low or high H_2:

$$V_P = P \exp\left(-0.5 \left[\frac{\Delta ECP + ECP_{OS}}{\lambda} \right]^2 \right) \qquad \textbf{Eq. 2-3}$$

where: V_P = velocity relative to the peak height (e.g., 1-8)

P = height of peak (e.g., 3-8X)

λ = width of peak = 20.2 (Alloy 82 weld metal) or 35.6 (Alloy 600)

ECP_{OS} = offset of CGR peak from Ni/NiO phase boundary (or ΔECP_0)

ΔECP = H_2 value vs. peak H_2

$$\Delta ECP = 29.58 \left(\frac{T(^\circ C) + 273.2}{298.2} \right) \cdot \log \left(\frac{H_2}{H_2\,(peak)} \right) \qquad \textbf{Eq. 2-4}$$

For example, the ΔECP for 80 cc/kg at 325°C is 29.58 * 598.2/298.2 * log (80/10.4) = 52.6 mV.

The parameters in Equation 2-3 are given by Attanasio and Morton [3] and shown in Table 2-2. Because the nature of their formulation is that at large ΔECP (very low or high H_2) the CGR (V_P) approaches 0 rather than 1, they restricted the range of applicability of the fit (Table 2-2). Figures 2-7, 2-8, and 2-9 show that the Attanasio and Morton formulation approaches 0 and thereby does not accurately reflect the nature of the off-peak CGR data.

Table 2-2
Fitting / Modeling Parameters for Various Materials (copy of Table 6 from Reference 3)

Test Material and Condition	$\frac{SCCGR_{max}}{SCCGR_{min}}$	ΔECP_o	λ	Range of Applicability[†]
EN82H, 338°C	8.09	10.5	20.2	- 52 mV < ΔECP < 31 mV
Alloy 600, 338°C	2.81	- 10.2	35.6	- 41 mV < ΔECP < 61 mV
Alloy X-750 HTH, 360°C	4.89	4.2	20.4	- 41 mV < ΔECP < 32 mV
Alloy X-750 AH, 338°C	7.19	30.8	40.0	- 110 mV < ΔECP < 49 mV

Notes:
Column 2 is the CGR peak
Column 3 is the ECP offset (ECP_{OS} or ΔECP_0) from the Ni/NiO phase boundary
Column 4 is the width parameter; the full width at half max is ~2.375X * λ
Column 5 is the range of applicability in the Attanasio and Morton formulation

We have chosen to reformulate their model in a fashion that retains their parameters (see the descriptions following Equation 2-3) but causes the model to approach 1 at very low or high H_2 while retaining the fit near the CGR peak:

$$V_P = (P-1)\exp\left(-0.5\left[\frac{\Delta ECP + ECP_{OS}}{\lambda + (0.46)^{1/P}}\right]^2\right)+1 \qquad \textbf{Eq. 2-5}$$

Figure 2-15 compares the two formulations. Because Equation 2-5 provides a good fit to the CGR data away from the peak (e.g., Figures 2-7, 2-8, and 2-9), there is a strong basis for its use at any arbitrary H_2 level, although if calculations well away from the peak become important, more CGR data should be generated in these regions to verify the response.

[†] The SCC CGR effect of dissolved H_2 seems to have an appreciable influence in a narrow range of ECP near the Ni/NiO phase transition.

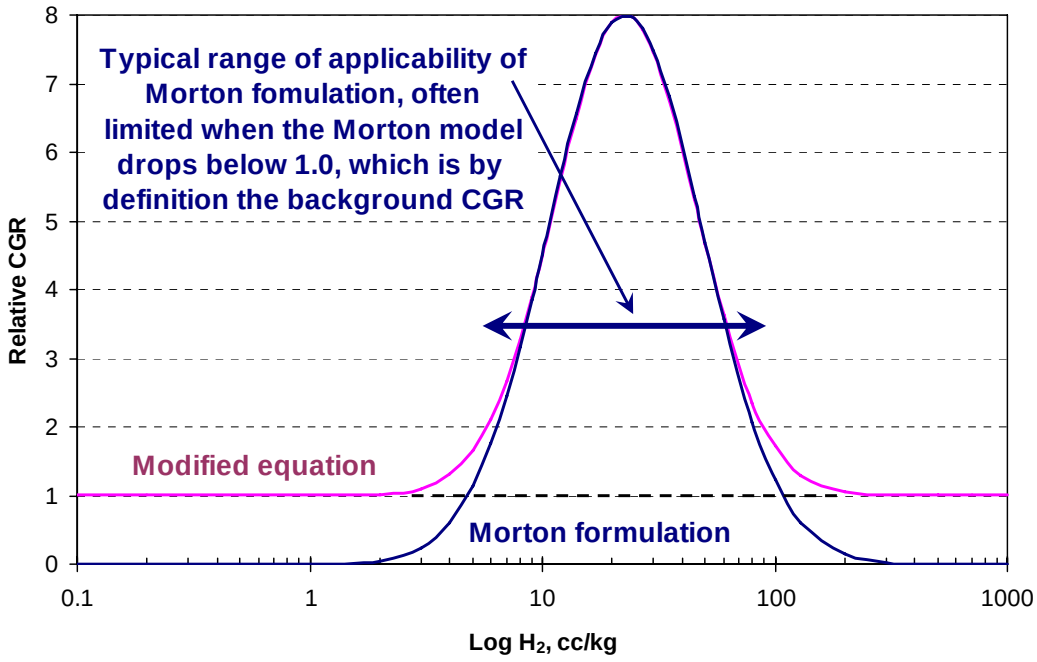

Figure 2-15
Comparison of the Attanasio and Morton Model Formulation and a Modified Model

Note:
The original formulation drops to zero growth rate at extremes of H_2, whereas by definition it should drop to 1.0. The range of applicability of the original model is primarily limited by the point where it drops below 1.0. While there is not always data at extremes of H_2, it is reasonable to assume that the growth rate approaches 1.0 as the H_2 is raised or lowered. The two models deviate very little in the range of applicability used by Attanasio and Morton [3].

There are also issues related to the *offset* in ECP/H_2 (ECP_{OS}) and *width* of the CGR peak. Attanasio and Morton (Table 2-2) simply fitted the data to their model (Equation 2-3) and listed the best-fit parameters. However, it seems fundamentally unlikely that Alloy 600 would exhibit a –10.2 mV *offset* while Alloy 82 would exhibit a +10.5 mV *offset* and Alloy X-750 HTH a 4.2 mV *offset*, especially since a quick evaluation of the data in Figures 2-7, 2-9, and 2-10 shows that there is little or no basis for concluding that all the CGR peaks do not actually occur at the Ni/NiO phase boundary itself. Morton concurs with this conclusion [7]. Thus the working approach in the analyses presented in this report is that no ECP *offset* exists for these materials. Alloy X-750 AH (Figure 2-8) is less clear – with an indicated *offset* of 30.8 mV, it's harder to rationalize that a 0 mV *offset* applies, although it should be noted that there is only a single data point on the low H_2 side of the CGR peak.

The *width* values in the Attanasio and Morton model (Table 2-2) have been retained, although if one compares the data in Figures 2-7 and 2-9, a case can be made that the peak *widths* may not actually be very different. Despite the remarkable efforts of Morton and colleagues, resolving such uncertainties would require quite a bit more experimental work. While 10 mV variations in *offset* or 20 mV variations in *width* may seem like small differences, they do in fact have moderate effects on the model predictions for CGRs in PWR components.

Some additional details of the effects of the *offset* and *width* parameters in the present model are provided in Appendix A. In summary, the following adjustments have been made to the published Attanasio and Morton model [3]:

1. The model has been reformulated (Equation 2-5) to approach a CGR of 1 (the baseline growth rate at very low or very high H_2) rather than 0, while retaining the Attanasio and Morton parameters and shape over most of the peak.
2. The *offset* in ECP/H_2 (ECP_{OS})is assumed to be 0 for most Ni alloys (no predictions for Alloy X-750 AH are made in this report, so the issue of its *offset* is for now moot, although we would be inclined to retain its *offset*).
3. The range of applicability in ECP/H_2 has been expanded to any value of H_2 because of the reformulation of the model.
4. The range in H_2 wherein fully thermodynamic ECP response is assumed is also expanded, to at least as low as 0.1 cc/kg H_2 in pure water or B/Li environments.

For reference, the effect of temperature activation on CGR is calculated as follows:

$$V_R = e^{-\frac{Q}{R}\left(\frac{1}{T1}-\frac{1}{T2}\right)} \qquad \text{Eq. 2-6}$$

where: V_R = the ratio of the CGRs at one temperature (T2) vs. another (T1)

Q = activation enthalpy, 130,000 J/mole

R = molar gas constant, 8.314 J/mole-K

T = temperature in K (°C + 273.2)

For example, relative to 290°C, the CGR at 343°C is exp(–130000/8.314 * (1/616.2 – 1/563.2)), or 10.9X higher.

2.4 Prediction of the Effect of Changes in H_2 on PWSCC CGRs in Nickel-Base Alloys

The CGR peak response in the vicinity of the Ni/NiO phase boundary as shown schematically in Figure 1-3 implies a simpler situation than actually exists when evaluating PWSCC mitigation for nickel-base alloys. Considering first the relationship between H_2 fugacity and the Ni/NiO phase boundary, the following primary factors must be recognized:

- The effect of temperature on the H_2 fugacity coefficient (Figure 2-1). This means that a given solution will have a reduced H_2 fugacity as it is heated, even though the H_2 concentration remains constant.
- The change in the thermodynamic properties of Ni and NiO vs. temperature.

These factors lead to a power law relationship between H_2 fugacity and temperature in defining the location of the Ni/NiO phase boundary (Equation 2-2 and Figures 1-4 and 1-5), with less H_2 needed for Ni metal stability at lower temperatures.

There are additional considerations associated with the expected peak in SCC growth rate near the Ni/NiO phase boundary, and the following further factors must also be recognized:

- Different alloys, heats and test conditions (e.g., temperature and stress intensity factor) yield a different "baseline" crack growth rate. Higher stress intensity factors, higher temperature and higher-strength materials (such as alloy 182 or 82 weld metals) lead to higher growth rates. However, there is reasonable evidence to indicate that the FOI for a given change in H_2 is not strongly dependent on material heat or stress intensity.
- All nickel-base alloys show a similar effect of temperature (activation enthalpy), with higher growth rates at elevated temperature. Relative to 290°C, the crack growth rate is about 5X higher at 325°C and 10X higher at 343°C (based on the recognized activation enthalpy of 130 kJ/mole). The effect of H_2, including the height of the CGR peak, is not consequentially affected by temperature over the range of (at least) 260 to 360°C.
- The height of the CGR peak vs. H_2 fugacity has a strong effect on the FOI that is expected for a given change in H_2 level. The width of the peak may also vary somewhat from material to material, but this generally has a somewhat smaller effect (see Section 2.3 and Appendix A).
- There is an indication that a small offset from the Ni/NiO phase boundary might exist in the H_2 / corrosion potential value where the CGR peaks, but this is uncertain. The tabular and graphed data in the main section of this report do not use an ECP offset, i.e., the CGR peak is assumed to occur at the Ni/NiO phase boundary (see Section 2.3 and Appendix A).

When integrating these parameters across many materials and many temperatures, the determination of an expected FOI associated with a specific change in H_2 is not trivial and will be unique to each specific case. For example, if the reference condition is 35 cc/kg H_2, reducing H_2 to lower values will result in moving closer to the peak in crack growth rate at all relevant temperatures. The peak growth rate occurs at ~16.5 cc/kg at 343°C, at ~10.4 cc/kg at 325°C and ~4.3 cc/kg at 290°C.

So, if a component weld or test specimen made, e.g., of alloy 182 is exposed to 343°C water with 35 cc/kg H_2, the effect of changing H_2 on CGR should be approximately as shown in Figure 2-16 (Note that the CGR values in these figures are assumptions loosely derived from the MRP-115 / MRP-55 databases for alloys 182 / 600, respectively and corrected appropriately for temperature). If H_2 is decreased, there will be an initial increase in growth rate, then a decrease, with the growth rate dropping below its initial value (at 35 cc/kg) only below 7.7 cc/kg H_2. If H_2 is increased, a monotonic decrease in growth rate is expected.

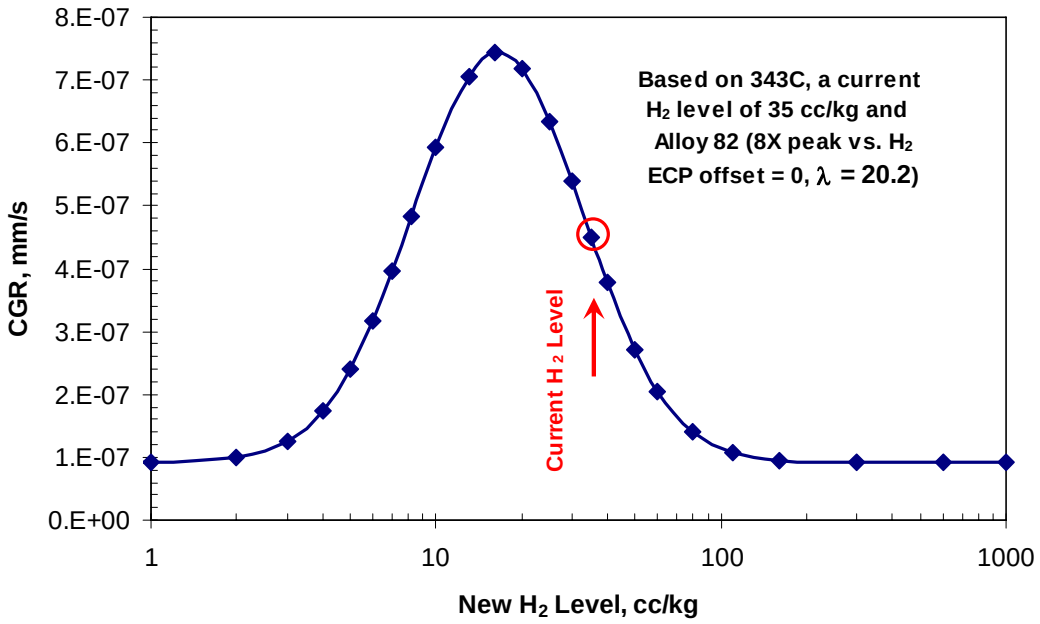

Figure 2-16
Predicted Effect of H_2 on the Crack Growth Rate of Nickel-Base Alloys with an Assumed "8X Peak" at 343°C

Note:
The red circle represents a hypothetical case where the current H_2 level is 35 cc/kg. Shifting to higher H_2 will monotonically decrease the growth rate, whereas shifting to lower H_2 will initially increase the growth rate, then (below ~16.5 cc/kg H_2) decreases the growth rate. No benefit will occur until the H_2 level is below ~7.7 cc/kg H_2.

The picture at lower temperatures is somewhat different because the peak growth rate occurs at a lower H_2 fugacity – indeed, 35 cc/kg H_2 is well above the CGR peak (Figure 2-17). If H_2 is decreased, the growth rate should increase markedly before the peak is encountered and the growth rate begins to decrease. A net benefit in growth rate (relative to 35 cc/kg H_2) is only expected once the H_2 is below ~3.1 cc/kg H_2 at 325°C and below ~0.52 cc/kg H_2 at 290°C. Conversely, the anticipated benefit of moving to higher H_2, although always present, is reduced at lower temperatures (compared to 343°C) because the initial H_2 fugacity is already well above the CGR peak. Tables 2-3 and 2-4 shows the predicted benefit of various changes in the H_2 operating point for two categories of materials and at four temperatures. Table 2-3 uses 35 cc/kg H_2 as the baseline for most comparisons, while Table 2-4 uses 30 cc/kg H_2. While many PWRs currently operate at 35 cc/kg H_2, 30 cc/kg H_2 represents a relevant condition for some PWRs. Also, some 35 cc/kg H_2 plants used to operate at lower H_2, and observed PWSCC reflects the time (and higher growth rates) associated with their operation, e.g., at 30 cc/kg H_2. Thus, 30 cc/kg H_2 is a useful baseline condition for many PWRs.

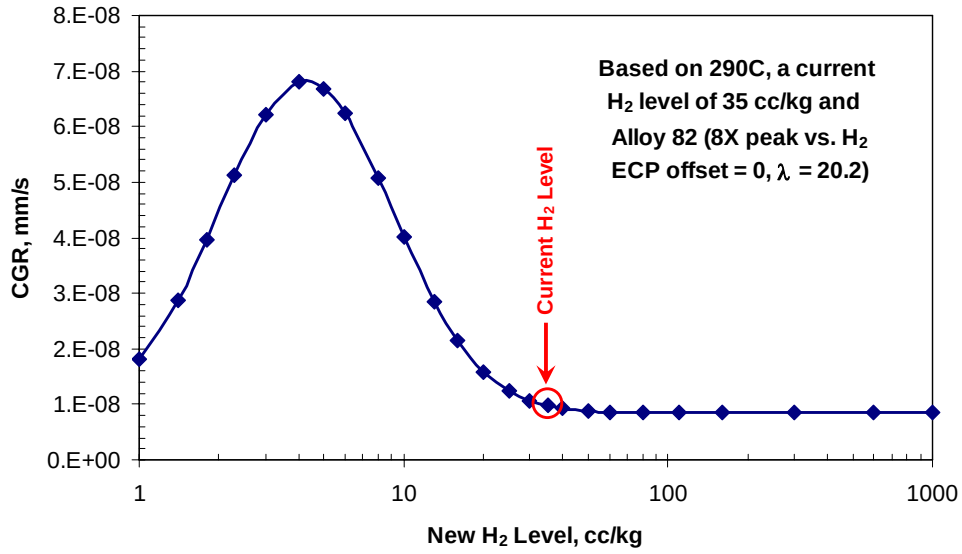

Figure 2-17
Predicted Effect of H_2 on the Factor of Improvement in Crack Growth Rate of Nickel-Base Alloys with an Assumed "8X Peak" at 290°C

Note:
The red circle represents a hypothetical case where the current H_2 level is 35 cc/kg. Shifting to higher H_2 will monotonically decrease the growth rate, whereas shifting to lower H_2 will initially increase the growth rate, then (below ~4.3 cc/kg H_2) decrease the growth rate. No benefit occurs until the H_2 level is below ~0.52 cc/kg H_2.

Table 2-3
Factors of Improvement for Various Materials, Temperatures, and Changes in Operating H_2

H_2 at Ni/NiO	Alloy 600 (3X Peak Height, λ = 35.6, ECP_{os} = 0)				Alloy 182/82 (8X Peak Height, λ = 20.2, ECP_{os} = 0)			
	290°C	310°C	325°C	343°C	290°C	310°C	325°C	343°C
	4.3 cc/kg	7.1 cc/kg	10.4 cc/kg	16.5 cc/kg	4.3 cc/kg	7.1 cc/kg	10.4 cc/kg	16.5 cc/kg
35 → 100	1.30	1.53	1.69	1.76	1.14	1.62	2.52	3.94
35 → 80	1.27	1.44	1.55	1.56	1.14	1.59	2.36	3.22
35 → 50	1.14	1.20	1.22	1.19	1.10	1.37	1.63	1.66
35 → 10	0.54	0.58	0.68	0.91	0.24	0.23	0.33	0.76
35 → 3	0.47	0.69	1.02	1.67	0.16	0.37	1.04	3.63
35 → 1	0.72	1.21	1.74	2.41	0.54	1.37	2.55	4.84
50 → 100	1.14	1.27	1.39	1.47	1.03	1.18	1.54	2.37
50 → 80	1.11	1.20	1.27	1.31	1.03	1.16	1.45	1.93

Notes:
Left column represents a proposed change in H_2 operating condition (emphasis on a baseline of 35 cc/kg H_2). The peak in crack growth rate is considered to be at the Ni/NiO phase boundary in all cases (ECP_{os} = 0). The *width* of the peak varies with material as per ref. [3]. Table entries below 1X indicate the change in H_2 is detrimental. Note that a baseline of 35 cc/kg H_2 reflects the current operating point for many PWRs, but 30 cc/kg H_2 represents a relevant condition for some PWRs. Also, some 35 cc/kg H_2 plants used to operate at lower H_2, and observed PWSCC reflects the time (and higher growth rates) associated with their operation, e.g., at 30 cc/kg H_2. Thus, 30 cc/kg H_2 is a useful baseline condition for many PWRs.

Table 2-4
Factors of Improvement for Various Materials, Temperatures, and Changes in Operating H_2

H_2 at Ni/NiO	Alloy 600 (3X Peak Height, λ = 35.6, ECP_{os} = 0)				Alloy 182/82 (8X Peak Height, λ = 20.2, ECP_{os} = 0)			
	290 °C	310 °C	325 °C	343 °C	290 °C	310 °C	325 °C	343 °C
	4.3 cc/kg	7.1 cc/kg	10.4 cc/kg	16.5 cc/kg	4.3 cc/kg	7.1 cc/kg	10.4 cc/kg	16.5 cc/kg
30 → 100	1.40	1.66	1.84	1.87	1.25	1.97	3.17	4.71
30 → 80	1.36	1.57	1.68	1.66	1.24	1.94	2.97	3.84
30 → 50	1.22	1.31	1.33	1.27	1.21	1.67	2.05	1.99
30 → 10	0.58	0.63	0.74	0.97	0.27	0.27	0.41	0.91
30 → 3	0.50	0.75	1.10	1.77	0.17	0.44	1.31	4.34
30 → 1	0.77	1.31	1.88	2.56	0.59	1.67	3.20	5.79
50 → 100	1.14	1.27	1.39	1.47	1.03	1.18	1.54	2.37
50 → 80	1.11	1.20	1.27	1.31	1.03	1.16	1.45	1.93

Notes:
Left column represents a proposed change in H_2 operating condition (emphasis on a baseline of 30 cc/kg H_2). The peak in crack growth rate is considered to be at the Ni/NiO phase boundary in all cases (ECP_{os} = 0). The *width* of the peak varies with material as per ref. [3]. Table entries below 1X indicate the change in H_2 is detrimental

While an expected FOI can be calculated for each temperature (e.g., Figure 2-18), this is somewhat misleading because there is also a large role of temperature activation on growth rate. It will usually be more important to achieve a reasonably low growth rate at all temperatures than to achieve a specific FOI. Figure 2-19 summarizes the expected effect of changes in H_2 fugacity on CGR at 290, 325 and 343°C for a nickel-base alloy that has an 8X peak in CGR; this figure provides the best basis for an overall comparison based on actual growth rate. It also shows that shifting to lower H_2 is an option that can potentially be considered to mitigate PWSCC – despite the fact that lowering H_2 down even as low as 1 cc/kg always produces a small increase in CGR at 290°C, the absolute values for growth rate at that temperature are generally much lower than at 325 and 343°C.

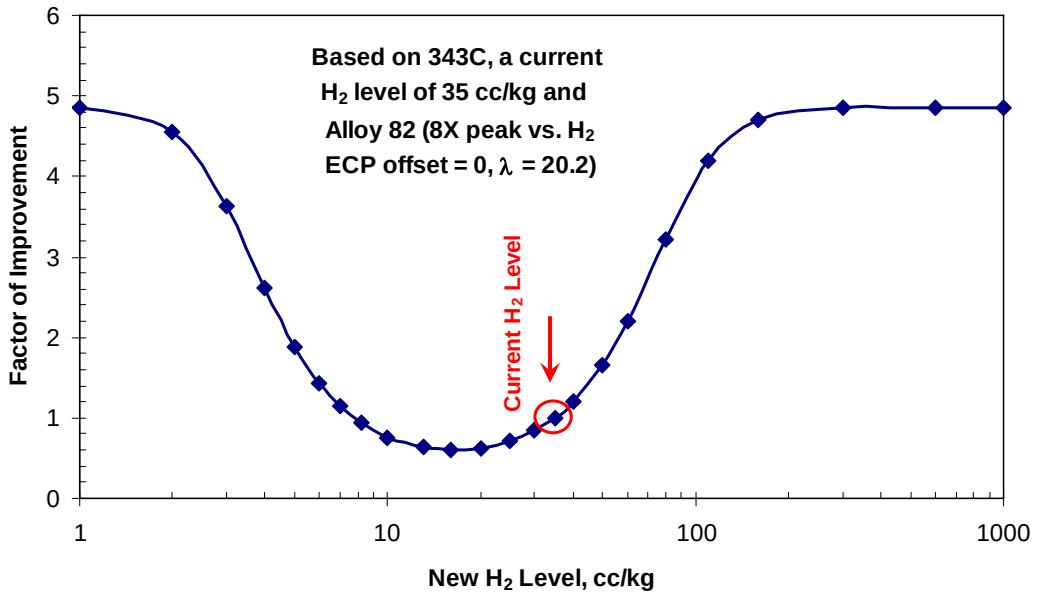

Figure 2-18
Predicted Effect of H_2 on the Factor of Improvement in Crack Growth Rate of Nickel-Base Alloys with an Assumed "8X Peak" at 343°C

Note:
The red circle represents a hypothetical case where the current H_2 level is 35 cc/kg. Shifting to higher H_2 will monotonically decrease the growth rate, whereas shifting to lower H_2 will initially increase the growth rate, then (below ~16.5 cc/kg H_2) decrease the growth rate. No benefit will occur until the H_2 level is below ~7.7 cc/kg H_2.

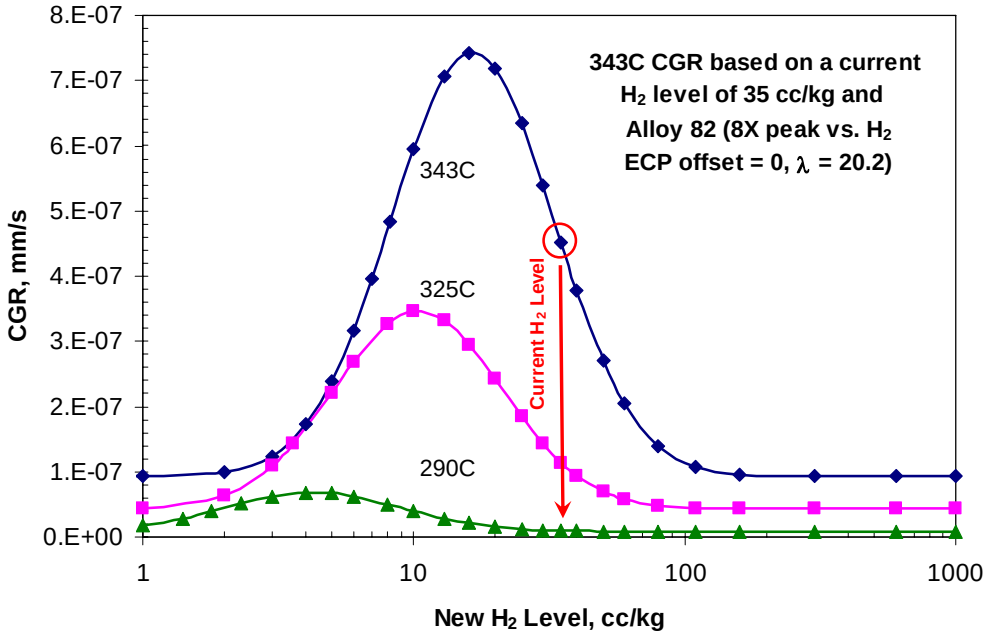

Figure 2-19
Predicted Effect of H_2 on the CGR of Nickel-Base Alloys with an Assumed "8X Peak" at 290, 325 or 343°C

Note:
The red circle and line represents a hypothetical case where the current H_2 level is 35 cc/kg. Shifting to higher H_2 will monotonically decrease the growth rate, whereas shifting to lower H_2 will initially increase the growth rate, and no benefit will occur until the H_2 level is below about 0.52, 3.1 and 7.7 cc/kg H_2 for 290, 325 and 343°C, respectively. While the peak height is 8X at all temperatures, the actual growth rate is much higher at 343°C.

Figure 2-20 presents the corresponding predictions for a nickel-base alloy that has a 3X peak in CGR vs. H_2 (e.g., Alloy 600). The actual peak height for all nickel-base alloys is not precisely known, but 2.5 – 3X is a solid estimate for Alloy 600 base metal. It is reasonable to assume it applies to other nickel alloy base metals, such as Alloy 690, but confirmation is needed. The same caveat applies to the 8X peak for nickel-base weld metals (e.g., Alloy 82); this value is assumed to apply also for Alloy 182 weld metal and other high strength nickel-base alloys (e.g., Alloy X-750 and Alloy 718), although peak heights are more commonly observed to be ~6X for Alloy X-750. Note that the peak height typically depends strongly on both the peak CGR (often defined only by one or two data points) as well as the baseline CGR at low and high H_2 (also often inadequately defined).

Figure 2-20 illustrates that the very positive effect of lower temperatures of operation may outweigh considerations of optimizing H_2 fugacity in terms of predicted CGRs for some Alloy 600 components.

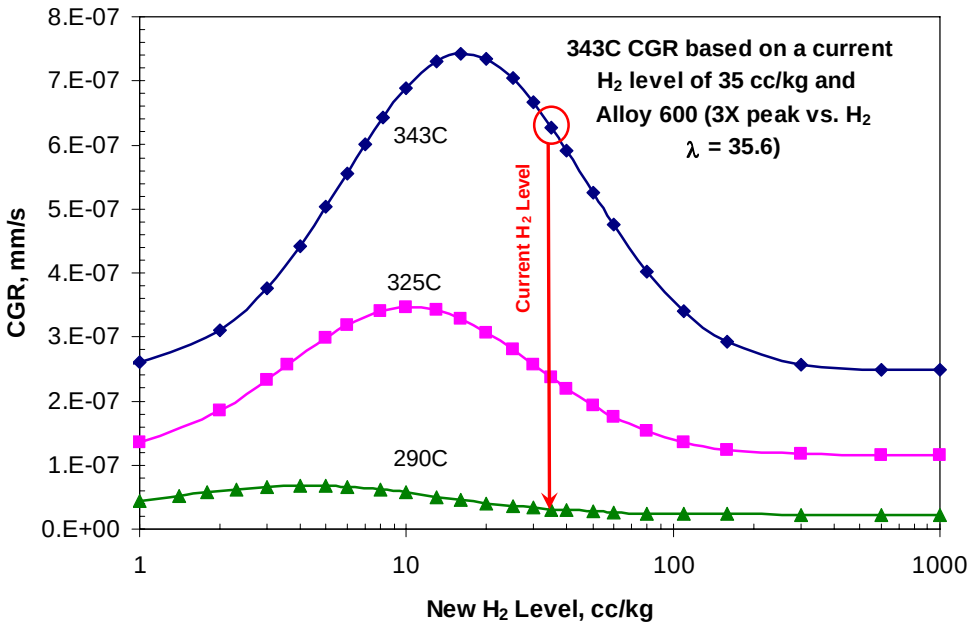

Figure 2-20
Predicted Effect of H_2 on the Crack Growth Rate of Nickel-Base Alloys with an Assumed "3X Peak" at 290, 325 or 343°C

Note:
The red circle and line represents a hypothetical case where the current H_2 level is 35 cc/kg. Shifting to higher H_2 will monotonically decrease the growth rate, whereas shifting to lower H_2 will initially increase the growth rate. No benefit will occur until the H_2 level is below about 0.52, 3.1 and 7.7 cc/kg H_2 for 290, 325 and 343°C, respectively. While the peak height is 3X at all temperatures, the actual growth rate is much higher at 343°C.

The predicted effect of H_2 on the SCC growth rate of Alloy 182 weld metal with an "8X peak" as a function of temperature is shown in Figure 2-21 for 25, 45 and 70 cc/kg H_2. Note that the observed CGRs vary with many factors, especially heat and stress intensity factor, but the effects of H_2 apply independent of these factors (and also apply to Alloy 82 weld metal). A decrease the growth rate occurs when shifting from 25 cc/kg H_2 to 45 or 70 cc/kg H_2. The peak height is 8X at all temperatures, but as temperature is changed there is an effect of the CGR activation energy (130 kJ/mole) as well as the change in the location of the CGR peak vs. H_2 (16.5 cc/kg H_2 at 343°C, 10.4 cc/kg at 325°C and 4.3 cc/kg at 290°C). From these data, a predicted factor of improvement for SCC growth rates of Alloy 82/182 weld metal can be calculated for changes in H_2 from 25 to 45 cc/kg H_2 and from 25 to 70 cc/kg H_2 as a function of temperature (Figure 2-22). The factor of improvement changes with temperature because of the change in the location of the CGR peak vs. H_2, with the largest benefits occurring where the slope of the CGR peak vs. H_2 is highest.

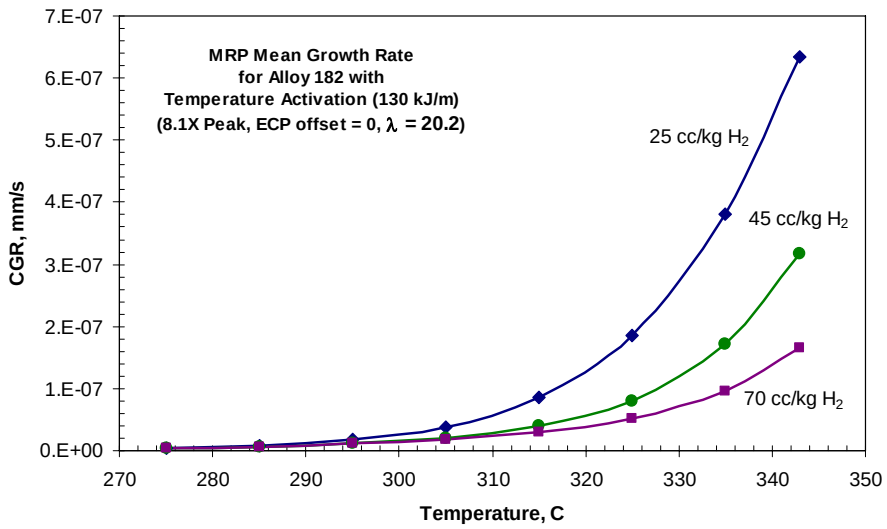

Figure 2-21
Predicted Effect of H_2 on the CGR of Alloy 182 Weld Metal with an Assumed "8X Peak" at 25, 45 and 70 cc/kg H_2 as a Function of Temperature

Note:
Shifting from 25 cc/kg H_2 to 45 or 70 cc/kg H_2 produces a decrease the growth rate. While the peak height is 8X at all temperatures, as temperature is changed there is an effect of the CGR activation energy (130 kJ/mole) as well as the change in the location of the CGR peak vs. H_2 (16.5 cc/kg H_2 at 343°C, 10.4 cc/kg at 325 ° and 4.3 cc/kg at 290°C).

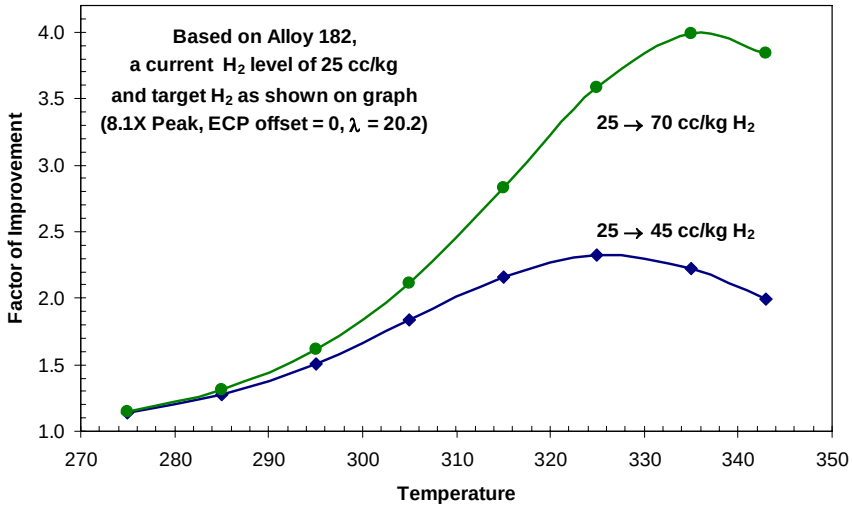

Figure 2-22
Predicted Effect of Factor of Improvement on the CGR of Alloy 182 Weld Metal with an "8X Peak" for Changes in H_2 from 25 to 45 cc/kg H_2 and 25 to 70 cc/kg H_2 as a Function of Temperature

Note:
The factor of improvement changes with temperature because of the change in the location of the CGR peak vs. H_2 (16.5 cc/kg H_2 at 343 °C, 10.4 cc/kg at 325° and 4.3 cc/kg at 290°C).

There are a variety of subtle complexities and potential additional issues that cannot be fully addressed here, although some are mentioned in Appendix A.

2.5 MRP Test Data on Influence of H_2 Fugacity on PWSCC CGRs in Nickel-Base Alloys

For just over two years, the MRP has sponsored a test program at GE-GRC that, while limited in scope compared to the literature data discussed earlier, attempts to confirm the above predictions of CGR by means of on-line monitoring for the effects of changes in H_2 fugacity on PWSCC. Examples of the data being obtained for a moderately susceptible heat of Alloy 600 have already been shown in Figures 2-13 and 2-14. The focus to date has been on increasing H_2 fugacity in steps up to a maximum value of 80 cc/kg. In almost all cases studied, there has been a short-term decrease in the measured CGR that greatly exceeds the expected response (see Figure 2-23). Over longer periods of time, the CGRs sometimes rise again, and there is some scatter in the observations from specimen-to-specimen and test-to-test. It is known that the short term observation of a higher-than-expected reduction in growth rate when increasing H_2 can be attributed to the creation of a current-shorting path in the wake of the crack because of the formation of Ni-metal, and this again highlights the need for patience in measuring a steady-state, baseline CGR before making a change. Figure 2-24 shows that a reduction in long-term CGR equal to or greater than the predicted ratio for the step change in H_2 fugacity was obtained in 9 out 16 cases and the average of these data from duplicate specimens is in good agreement with the prediction.

Overall the data obtained to date provide a good confirmation of the expected benefit of increasing H_2 fugacity for Alloy 600 CGRs. Attention is now shifting in 2007 to examining the larger benefits expected for Alloy 182 weld metal. Furthermore, an attempt will be made to investigate the potentially synergistic effects of optimizing H_2 and adding Zn to primary water.

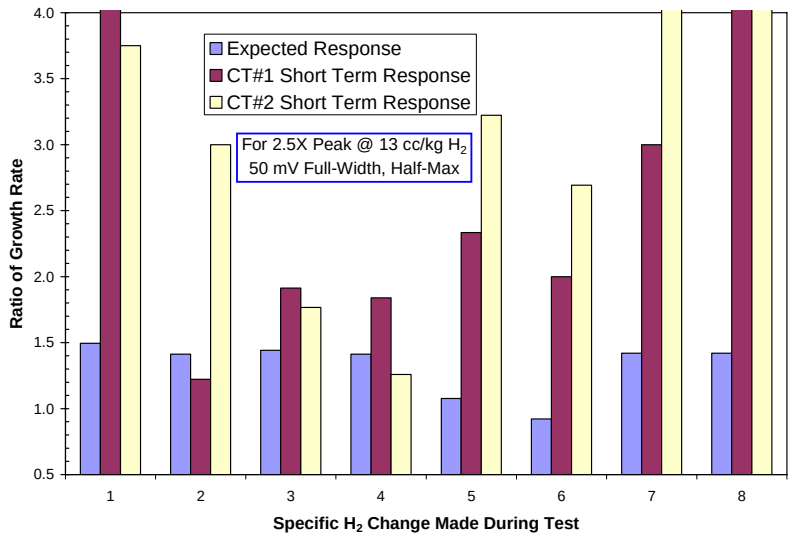

Figure 2-23
Comparison of Actual Short-Term Response of Duplicate CGR Specimens and Expected Effect for Various Step Changes in H_2 Fugacity, from Current MRP Test Program at GE-GRC

Note:
The overall ratio of observed-to-predicted CGR response is 2.9X in these short-term data.

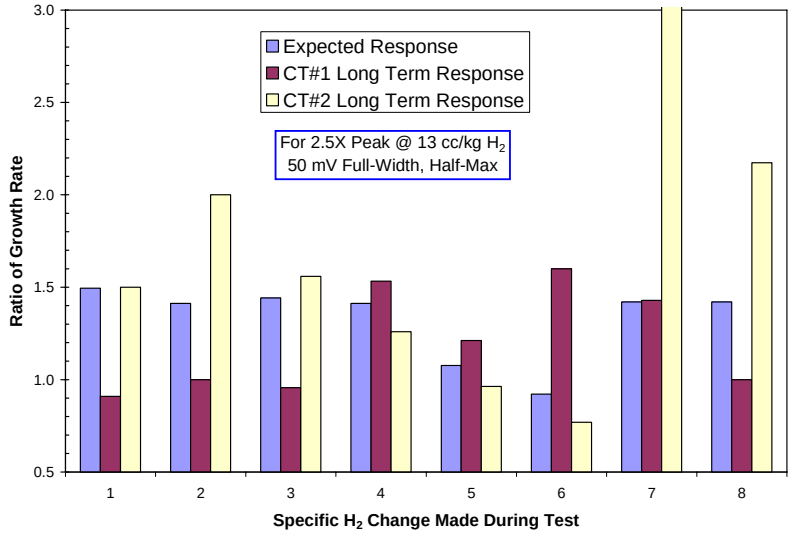

Figure 2-24
Comparison of Actual Long-Term Response of Duplicate CGR Specimens and Expected Effect for Various Step Changes in H_2 Fugacity, from Current MRP Test Program at GE-GRC

Note:
The overall ratio of observed-to-predicted CGR response is 1.1X in these long-term data, providing good confirmation of the KAPL results.

3
FURTHER MATERIAL-RELATED CONSIDERATIONS

The ongoing MRP test program focuses entirely on increasing H_2 fugacity to obtain lower CGRs. As mentioned previously, growth rates are also predicted to decrease at much lower H_2 levels, except for components operating at the lowest temperatures in the primary circuit. This alternative approach to optimizing H_2 fugacity is being investigated in Japan [14] and the emerging results from their program should be followed closely. Dropping much below 5 cc/kg H_2 raises the risk of radiolysis. For example, data (Figure 3-1) obtained using the proton irradiation at Harwell Variable Energy Cyclotron [15,16] indicates that only a limited increase in corrosion potential from radiolysis occurs in pure water at 288°C containing 200 ppb H_2 (2.2 cc/kg H_2). Therefore moving below the peak in crack growth rate of 4.3 cc/kg H_2 at 290°C seems unwise until more definitive data are identified or generated. Recent data from the Halden test reactor by Bennett et al. [17] in water containing only LiOH showed limited radiolysis at 1 cc/kg H_2. The increase in crack growth rate for stainless steels or nickel-base alloys that would result from a significant elevation of corrosion potential is dramatically larger (Figure 3-2) than any benefit from adjusting H_2 fugacity, so a very high level of confidence is needed that radiolysis will not occur, not only under the nominal H_2 conditions, but also if there is any deviation from the H_2 set point or local boiling. Because of the more concentrated PWR primary chemistry, there is also concern for relatively small changes in corrosion potential. That is, it would be wrong conclude that even a 100 or 200 mV change in potential would be safe (changing from –500 mV_{she} to –300 mV_{she} in pure water generally has a small effect on SCC).

There is an emerging recognition that fracture toughness and fracture tearing resistance can be markedly affected by exposure to the operating environment. The term *fracture toughness* is used to represent rapid fracture, while *fracture tearing resistance* is used for dynamic loading, typically characterized in a J-R test. The environmental fracture concerns span operating temperatures (e.g., 290 – 343°C) to lower temperatures (<150°C) associated with plant shutdown. The fracture tearing resistance phenomenon is often referred to using the somewhat misleading terminology “Low Temperature Crack Propagation” (LTCP), which should be restricted to the observations by Grove and Petzold [18] of the rapid extension of a sharp, pre-existing crack via a H_2 embrittlement mechanism at constant load or K (i.e., without the need for dynamic straining). This whole area is currently under investigation by the MRP [19] and it is not yet clear how relevant the effects measured in the laboratory are to operating plants.

Some effect of dissolved H_2 on LTCP and fracture behavior exists, but it is not always consistently observed and the reduction in fracture tearing resistance can be severe, even at low H_2 levels. While PWR primary water may have reduced H_2 levels during a normal shutdown, there is still an elevated concentration of H in the metal, which may play a role in the fracture process.

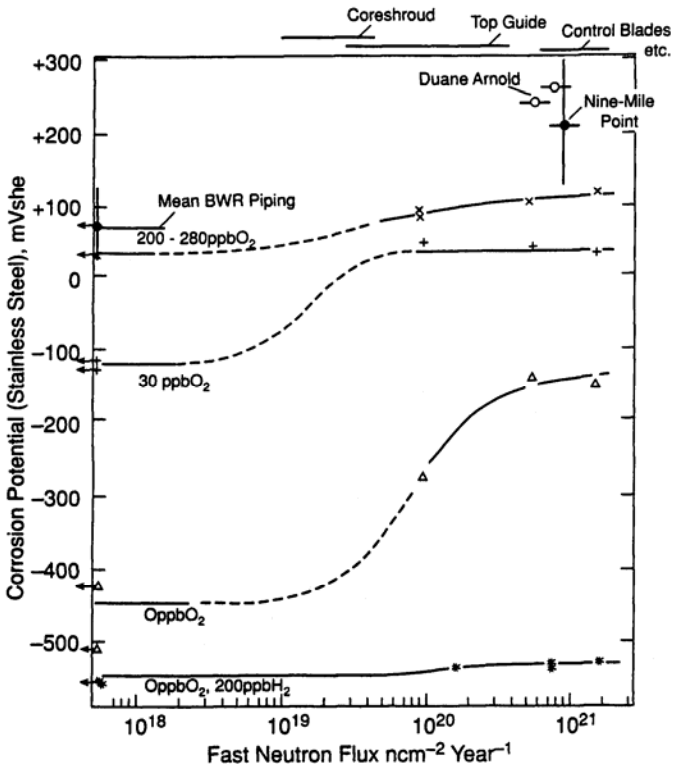

Figure 3-1
Corrosion Potential vs. Fast Neutron Flux for Stainless Steel in 288°C Water Containing Various Dissolved Gases and Concentrations

Note:
As the dissolved H_2 is increased from 0 to 200 ppb (2.2 cc/kg H_2), the role of radiolysis decreases, as reflected in the lack of an increase in corrosion potential. Experiments were performed using energetic protons at the Harwell Variable Energy Cyclotron, and the equivalent fast neutron flux calculated [15,16].

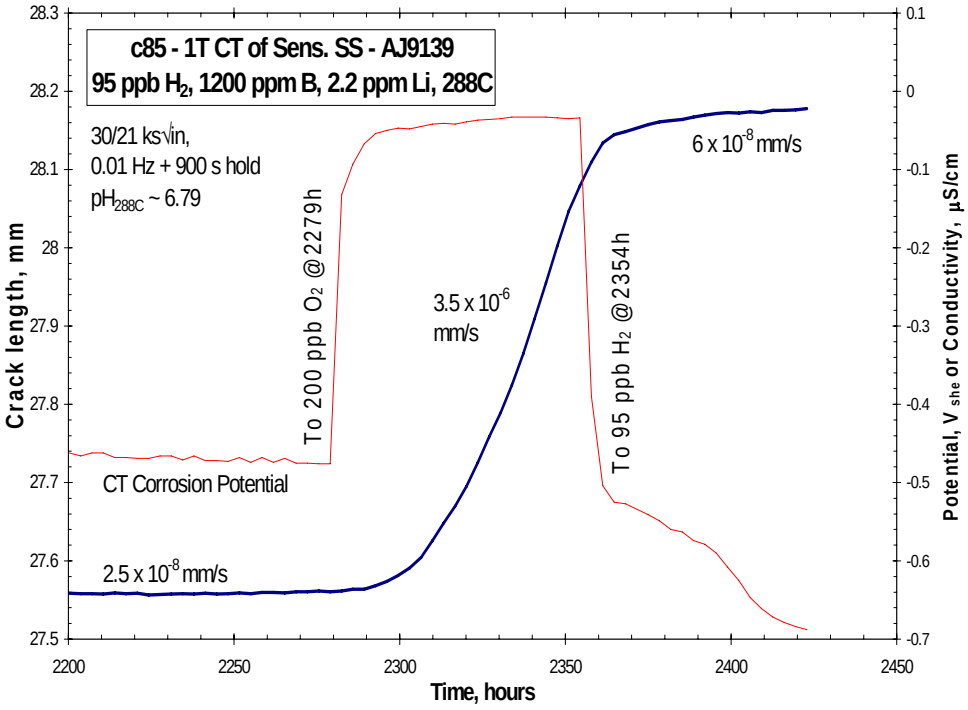

Figure 3-2
Crack Length vs. Time for Sensitized Type 304 Stainless Steel in 288°C Water Containing 1000 ppm B as H_3BO_3 and 1 ppm Li as LiOH

Note:
As the dissolved O_2 is increased from 0 to 200 ppb, the crack growth rate increases by ~100X, to a value that is much higher than is observed in pure water. From extensive data in 288°C water, such effects would also be observed on non-sensitized stainless steel and nickel-base alloys [5,20].

Given that H readily permeates through materials exposed in ~300°C water, and the nominal 35 cc/kg H_2 currently used is already a significant H_2 level, it is not clear that shifting to 2 – 3 X higher H_2 to mitigate PWSCC would consequentially increase the potential for LTCP and environmental effects on fracture to occur. Similarly, it is unlikely that such a change would influence the fracture toughness of nickel-base alloys exposed at high temperature to primary water. In both cases, however, it would be advisable to demonstrate the absence of negative effects in these areas conclusively as part of any qualification program.

4
CONCLUSIONS

There is a reasonable theoretical basis, supported in particular by extensive test data from the naval reactor program, to recommend moving to higher H_2 levels in PWR primary water to obtain partial mitigation of PWSCC for nickel-base alloys used in thick-wall components. Figures 2-19 and 2-20 show that such a change is expected always to have a positive effect in slowing down crack growth, independent of the material or operating temperature. Quantifying the predicted benefit of such a change for any particular component is complex because it depends on the material, the temperature, the starting H_2, the new H_2 target, and other factors. Overall, the absolute benefit of H_2 optimization will be greater at higher temperatures (e.g., in the pressurizer) because of the higher growth rate, and for higher-strength alloys (e.g. weld metals or alloy X750 vs. Alloy 600) because the CGR peak height is larger for these materials.

The MRP has in progress a modest test program intended to demonstrate the above effects. As discussed in Section 2-5, the results presently available support the beneficial effects of increasing H_2, but the use to date of Alloy 600 (where the predicted benefits of the chosen step changes in H_2 are relatively low) and specimen-to-specimen variations make the result less clear than desired. Testing will continue throughout 2007 and into 2008, focusing primarily on Alloy 182, and a full analysis of the data will be available in the first half of 2008. A small effort will be included to examine possible synergistic effects of adding Zn together with increasing H_2.

5
REFERENCES

1. P.L. Andresen, J.A. Wilson, K.S. Ahluwalia, "Use of Primary Water Chemistry in PWRs to Mitigate PWSCC of Ni-Base Alloys", Proc. Int. Conf. on Water Chemistry of Nuclear Reactor Systems, Korea, 2006.
2. P.L. Andresen et al., "Effects of PWR Primary Water Chemistry and Deaerated Water on SCC", Proc. 12th Int. Conf. on Environmental Degradation of Materials in Nuclear Power Systems – Water Reactors, TMS, 2006.
3. S.A. Attanasio and D.S. Morton, "Measurement of the Ni/NiO Transition in Ni-Cr-Fe Alloys and Updated Data and Correlations to Quantify the Effect of Aqueous Hydrogen and Primary Water SCC", Proc. 11th Int. Conf. on Environmental Degradation of Materials in Nuclear Power Systems – Water Reactors, ANS, 2003.
4. P. M. Scott and P. Combrade, "On the Mechanism of Stress Corrosion Cracking (SCC) Initiation and Growth in Alloy 600 Exposed to PWR Primary Water," Proc. 11th Int. Symp. on the Environmental Degradation of Materials in Nuclear Power Systems – Water Reactors, Stevenson, ANS, La Grange Park, IL, 2003.
5. P.L. Andresen, "Conceptual Similarities and Common Predictive Approaches for SCC in High Temperature Water Systems", Paper 96258, Corrosion/96, NACE, 1996. See also, P.L. Andresen, "Emerging Issues and Fundamental Processes in Environmental Cracking in Hot Water", Proc. Research Topical Symposium on Environmental Cracking, NACE, 2007.
6. D.S. Morton, S.A. Attanasio, and G.A. Young, "Primary Water SCC Understanding and Characterization Through Fundamental Testing in the Vicinity of the Nickel / Nickel Oxide Phase Transition", Proc. 10th Int. Conf. on Environmental Degradation of Materials in Nuclear Power Systems - Water Reactors, NACE, 2001.
7. Personal communication with D.S. Morton, March 2007.
8. J. Alvarez, R. Crovetto and R. Fernandez-Prini, "The Dissolution of N_2 and of H_2 in Water from Room Temperature to 640 K", Ber. Bunsenges. Phys. Chem. 92, p.935-940, 1988.
9. "Effects of Hydrogen, pH, Lithium and Boron on Primary Water Stress Corrosion Crack Initiation in Alloy 600 for Temperatures in the Range 320 – 330 °C", (MRP-147), EPRI, Palo Alto, CA: 2005. 1012145.
10. E. Richey, D.S. Morton and M.K. Schurman, "SCC Initiation Testing of Nickel-Based Alloys Using In-Situ Monitored Uniaxial Tensile Specimens", Proc. 12th Int. Conf. on Environmental Degradation of Materials in Nuclear Power Systems – Water Reactors, TMS, 2006.
11. S.A. Attanasio and D.S. Morton, "Measurement and Calculation of Electrochemical Potentials in Hydrogenated High Temperature Water, Including an Evaluation of the Yttria-Stabilized Zirconia/Fe/Fe_3O_4 Probe as a Reference Electrode", Paper 02517, Corrosion/05, NACE, 2005.

12. G.A. Young et al., "The Stress Corrosion Crack Growth Rate of Alloy 600 Heat Affected Zones Exposed to High Purity Water", NUREG/CP-0191: Proceedings of the NRC Conference on Vessel Penetration Inspection, Crack Growth and Repair, Gaithersburg, MD, 2003.
13. D.J. Paraventi and W.C. Moshier, "The Effect of Cold Work and Dissolved Hydrogen in the Stress Corrosion Cracking of Alloy 82 and Alloy 182 Weld Metal", Proc. 12th Int. Conf. on Environmental Degradation of Materials in Nuclear Power Systems – Water Reactors, TMS, 2006.
14. Presentations made in 2006 to the MRP by the Japan Atomic Power Company.
15. P.L. Andresen, F.P. Ford, J. Patrick Higgins, Isao Suzuki, Masakuni Koyama, Mamoru Akiyama, Tadatsune Okubo, Yoshitsugu Mishima, Shigeo Hattori, Hideo Anzai, Horikyuki Chujo, Yasushi Kanazawa, "Life Prediction Of Boiling Water Reactor Internals", Proc., ICONE-4 Conference, ASME, 1996.
16. P.L. Andresen, "Irradiation Assisted Stress Corrosion Cracking", in Book on Stress Corrosion Cracking: Materials Performance and Evaluation, Ed. R.H. Jones, ASM, Materials Park, 1992, p.181-210.
17. P.J. Bennett, M.A. McGrath, K. Bagli and M. Dymarski, "Measurements of Carbon Steel ECP and Critical Deuterium Concentration Under CANDU Conditions in the Halden Reactor", Proc. 12th Int. Conf. on Environmental Degradation of Materials in Nuclear Power Systems – Water Reactors, TMS, 2006.
18. C.A. Grove and L.D. Petzold, "Mechanism of SCC of Alloy X750 in High Purity Water", J. of Materials for Energy Systems, Vol. 7, No. 2, p.147-162, Sept 1985. See also L.D. Petzold and C.A. Grove, "Mechanism of SCC of Alloy X750 in High Purity Water", Proc. of Corrosion of Nickel Alloys, Ed. R.C. Scarberry, ASM, 1985, p.165.
19. A. Demma et al., "Low Temperature Crack Propagation Evaluation in Pressurized Water Reactor Service", Proc. 12th Int. Conf. on Environmental Degradation of Materials in Nuclear Power Systems – Water Reactors, TMS, 2006 and ongoing MRP presentations.
20. P.L. Andresen et al. "Stress Corrosion Crack Growth Rate Behavior of Ni Alloys 182 and 600 in High Temperature Water", Corrosion/02, Paper 02510, NACE, 2002.

A
DETAILED FACTORS IN THE CALCULATION OF H_2 EFFECTS ON SCC CGR

This appendix is included to clarify some of the details of the modeling and calculation of H_2 effects on SCC growth rates, particularly the role of the parameters that account for the possible effects of an *offset* from the Ni/NiO phase boundary and the *height* and *width* of the peak. Table 2-2 (which is a copy of Table 6 in reference [3]) represents the statistical best fit to their available data, but as is apparent from Figures 2-7, 2-8, and 2-9, it is unclear that any *offset* from the Ni/NiO phase boundary is justified (see discussion in Section 2-3).

The effect of a +10.5 mV (for Alloy 82 weld metal) or –10.2 mV (for Alloy 600) *offset* from the Ni/NiO phase boundary is not small – each represents about a 1.5X change in H_2, so that between them, there is a 2.25X difference. It appears that the +30.8 mV *offset* for Alloy X750 AH *might* be justified (Figure 2-8), but more data are needed at low H_2.

The *width* of the CGR peak also appears to vary, but the limited *height* of the CGR peak for Alloy 600 adds some uncertainty in the confidence associated with the *width* estimates. It is certainly possible that Alloy 600 possesses the same *width* as Alloy 82 and Alloy X750 HTH. Even the *width* of Alloy X750 AH is controlled strongly by the two round points, the high point at about +27 mV and the single point on the high H_2 side of the peak at –55 mV. Indeed, even the peak *heights* have uncertainly related not only to the highest (peak) crack growth rates that are observed (it is not uncommon for SCC growth rates to differ by 2X in nominally identical tests), but also to the baseline growth rates, which must be obtained at very low and/or very high H_2 levels. Such extremes of H_2 are not always easy to achieve, because the peak CGR occurs at moderately high H_2 at 360°C (~ 25 cc/kg), and a good background point requires at least 10X lower or higher H_2, e.g., >250 cc/kg.

Presenting all of the possible variations and repercussions of using individual fitting parameters vs. using more common fitting parameters (i.e., assuming all materials have a CGR peak at the Ni/NiO phase boundary, and vary only in peak *height*) would require many more tables and graphs. The figures in the main part of the report do use individual fitting parameters, although it is not clear to the authors, nor Morton [7], that all of these are justified. The following examples provide a context for understanding the repercussions of individual vs. common fitting parameters:

1. Figures A-1 and A-2 and Tables A-1 and A-2 show a comparison of the CGR and FOI at 343°C for Alloy 82 (8X peak) for an *offset* $ECP_{OS} = 0$ vs. +10.5 mV. The $ECP_{OS} = +10.5$ mV biases all of the calculations by ~ 1.5X in H_2.
2. Figures A-3 and A-4 show a comparison of CGR and FOI at 343°C for Alloy 82 (8X peak) for a *width* parameter $\lambda = 20.2$ (used in the main report for Alloy 82) vs. $\lambda = 35.6$ (used in the main report for Alloy 600).

3. Figure A-5 shows a comparison of the CGR at 343°C for various ECP *offsets*, using an 8X peak and the same width parameter λ = 20.2 as used for Alloy 82 for comparison with Figures A-1 – A-4. ECP_{OS} are plotted for –10.2 mV(from Alloy 600 data) vs. 0 (Ni/NiO phase boundary) vs. = +30.8 mV (from Alloy X750 AH data). The ECP_{OS} = +30.8 mV biases these calculations by ~ 3.2X in H_2 from the Ni/NiO phase boundary.

Table A-1
Factors of Improvement for Various Materials, Temperatures, and Changes in Operating H_2 with ECP Offset

H_2 at Ni/NiO	Alloy 600 (3X Peak Ht, λ = 35.6, $\underline{ECP_{OS}}$ = –10.2)				Alloy 182/82 (8X Peak Ht, λ = 20.2, $\underline{ECP_{OS}}$ = +10.5)			
	290°C	310°C	325°C	343°C	290°C	310°C	325°C	343°C
	4.3 cc/kg	7.1 cc/kg	10.4 cc/kg	16.5 cc/kg	4.3 cc/kg	7.1 cc/kg	10.4 cc/kg	16.5 cc/kg
35 → 100	1.50	1.69	1.74	1.62	1.03	1.15	1.51	2.63
35 → 80	1.42	1.54	1.55	1.42	1.02	1.15	1.49	2.46
35 → 50	1.19	1.21	1.19	1.12	1.02	1.11	1.33	1.67
35 → 10	0.58	0.70	0.88	1.20	0.39	0.23	0.21	0.35
35 → 3	0.64	1.04	1.54	2.28	0.13	0.17	0.34	1.27
35 → 1	1.10	1.77	2.32	2.83	0.27	0.66	1.30	2.71
50 → 100	1.26	1.39	1.46	1.44	1.00	1.03	1.14	1.58
50 → 80	1.19	1.27	1.30	1.27	1.00	1.03	1.13	1.48

Notes:
Left column represents a proposed change in H_2 operating condition (emphasis on 35 cc/kg H_2 baseline). The peak in crack growth rate is *offset* (ECP_{OS}) from the Ni/NiO phase boundary as per ref. [3]. The *width* of the peak varies with material as per ref. [3]. Table entries below 1X indicate the change in H_2 is detrimental. Note that a baseline of 35 cc/kg H_2 reflects the current operating point for many PWRs, but 30 cc/kg H_2 represents a relevant condition for some PWRs. Also, some 35 cc/kg H_2 plants used to operate at lower H_2, and observed PWSCC reflects the time (and higher growth rates) associated with their operation, e.g., at 30 cc/kg H_2. Thus, 30 cc/kg H_2 is a useful baseline condition for many PWRs.

Table A-2
Factors of Improvement for Various Materials, Temperatures, and Changes in Operating H_2 with ECP Offset

H_2 at Ni/NiO	Alloy 600 (3X Peak Ht, λ = 35.6, $\underline{ECP}_{os}$ = –10.2)				Alloy 182/82 (8X Peak Ht, λ = 20.2, $\underline{ECP}_{os}$ = +10.5)			
	290 °C	310 °C	325 °C	343 °C	290 °C	310 °C	325 °C	343 °C
	4.3 cc/kg	7.1 cc/kg	10.4 cc/kg	16.5 cc/kg	4.3 cc/kg	7.1 cc/kg	10.4 cc/kg	16.5 cc/kg
30 → 100	1.63	1.83	1.85	1.66	1.05	1.27	1.82	3.33
30 → 80	1.54	1.67	1.65	1.46	1.05	1.27	1.80	3.11
30 → 50	1.29	1.31	1.27	1.15	1.04	1.23	1.60	2.10
30 → 10	0.63	0.76	0.93	1.24	0.40	0.25	0.26	0.44
30 → 3	0.70	1.13	1.64	2.34	0.13	0.19	0.41	1.60
30 → 1	1.19	1.91	2.47	2.91	0.27	0.73	1.56	3.42
50 → 100	1.26	1.39	1.46	1.44	1.00	1.03	1.14	1.58
50 → 80	1.19	1.27	1.30	1.27	1.00	1.03	1.13	1.48

Notes:
Left column represents a proposed change in H_2 operating condition (emphasis on 30 cc/kg H_2 baseline). The peak in crack growth rate is *offset* (ECP_{os}) from the Ni/NiO phase boundary as per ref. [3]. The *width* of the peak varies with material as per ref. [3]. Table entries below 1X indicate the change in H_2 is detrimental.

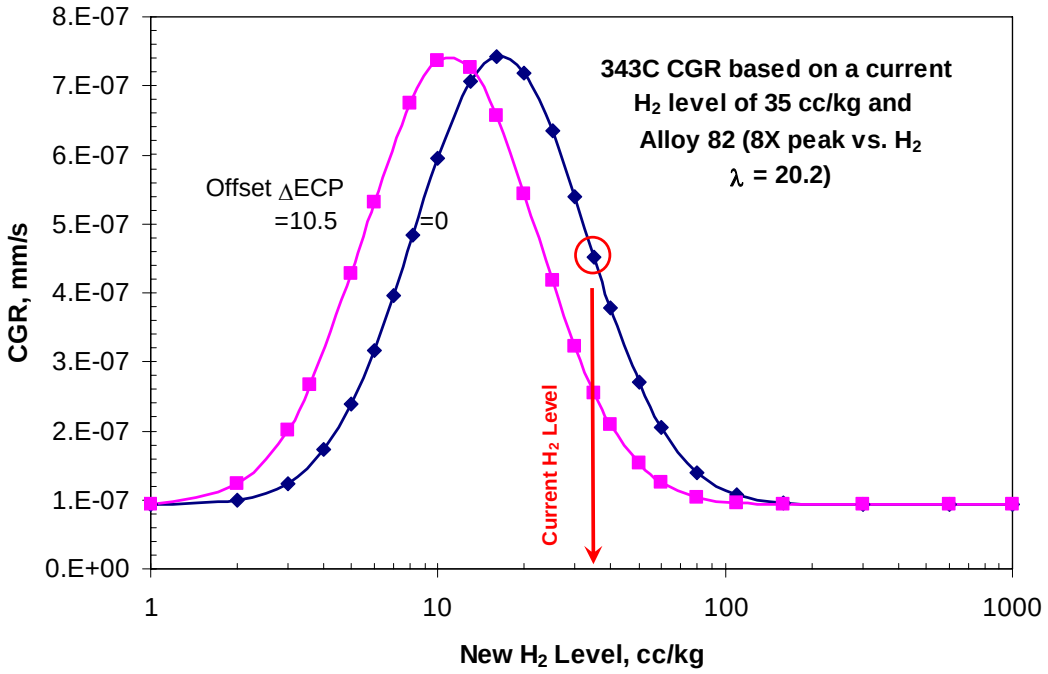

Figure A-1
Comparison of the Crack Growth Rate vs. H_2 at 343°C for Alloy 82 (8X Peak) for an *Offset* ECP_{os} = 0 vs. 10.5 mV.

The latter biases all of the calculations by ~1.5X in H_2.

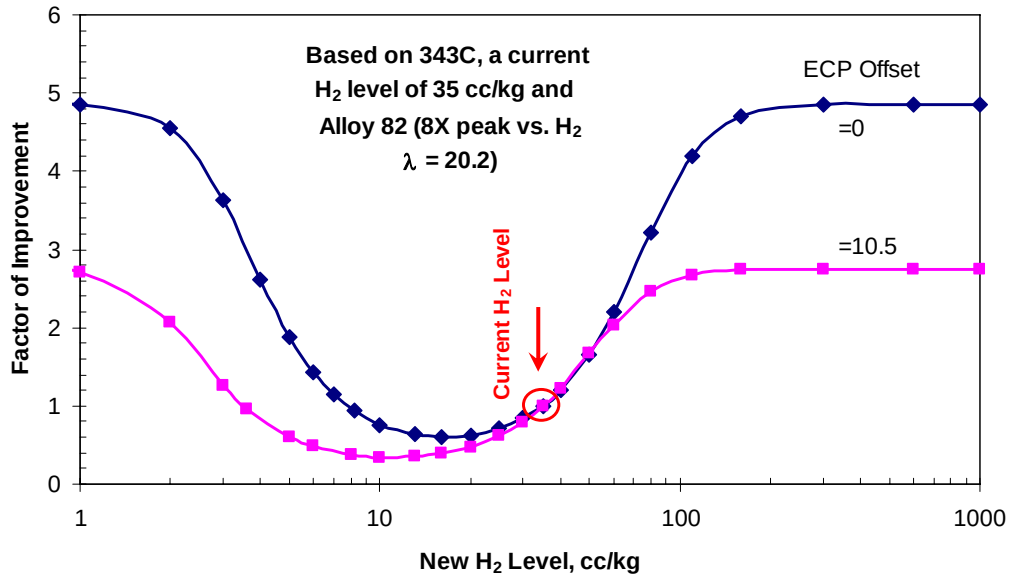

Figure A-2
Comparison of the Factor of Improvement vs. H_2 at 343°C for Alloy 82 (8X Peak) for an *Offset* ECP_{os} = 0 vs. 10.5 mV.

Note: The latter biases all of the calculations by ~1.5X in H_2. Note that the peak *height* remains the same, but the curve for ECP_{os} = 10.5 mV drops well below a FOI of 1.0, and its maximum FOI is only about 2.7X vs. 4.8X for the ECP_{os} = 0 curve.

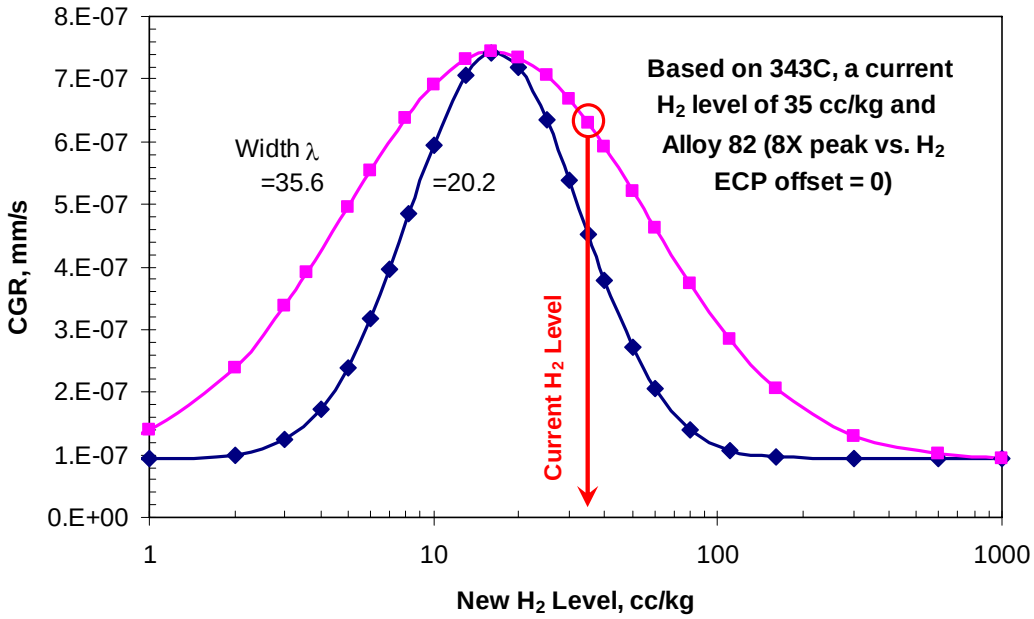

Figure A-3
Comparison of the Crack Growth Rate vs. H_2 at 343°C for Alloy 82 (8X Peak) for a Peak *Width* Parameter λ = 20.2 (used in main report for Alloy 82) vs. λ = 35.6 (used in main report for Alloy 600)

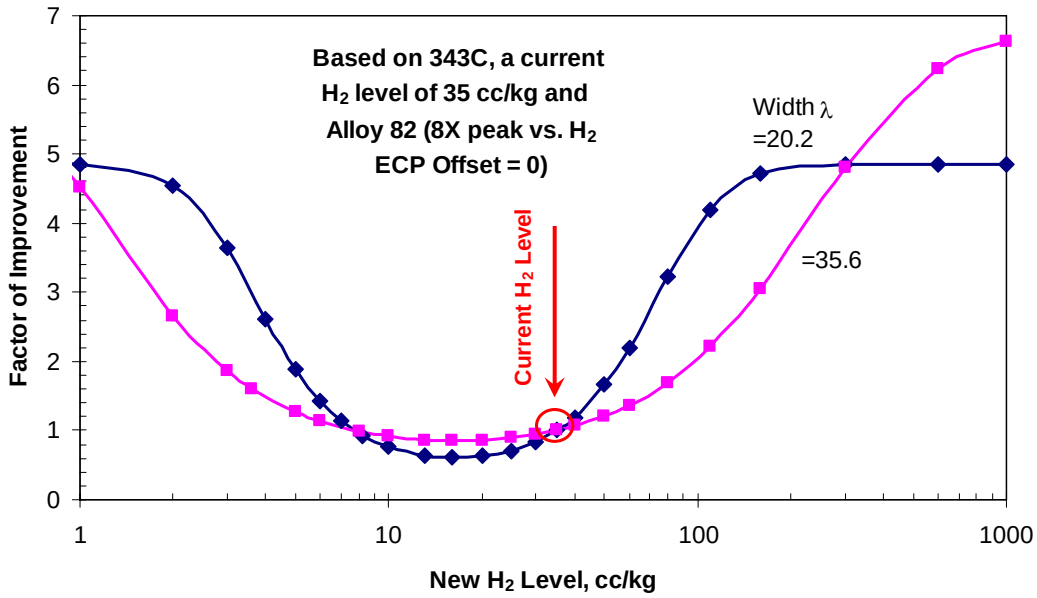

Figure A-4
Comparison of the Factor of Improvement vs. H_2 at 343°C for Alloy 82 (8X Peak) for a Peak *Width* Parameter λ = 20.2 (used in main report for Alloy 82) vs. λ = 35.6 (used in main report for Alloy 600)

Note: A broader peak for Alloy 82 is not proposed; it is shown only as an example of the effect of the peak width. At 343°C, the broader peak translates to less mitigation at achievable H_2 levels, but at lower temperatures, a greater mitigation opportunity would exist.

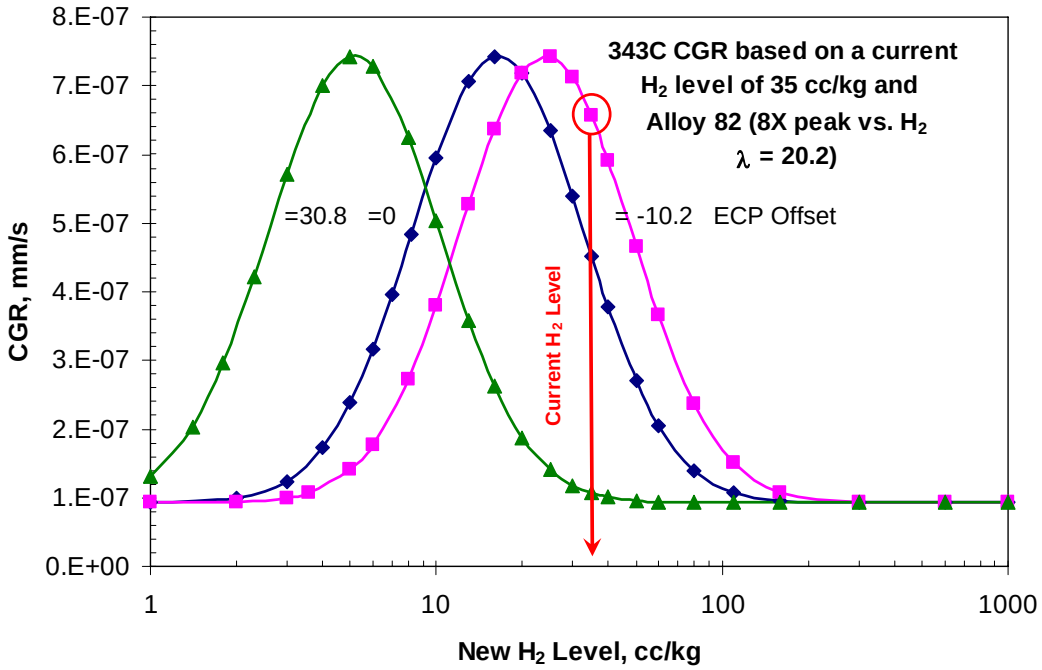

Figure A-5
Comparison of the CGR at 343°C for Various ECP Offsets, using an 8X Peak and the Same Width Parameter λ = 20.2 (for comparison with Figures A-2 – A-5)

Note: *Offset* ECP_{os} = - 10.2 (from Alloy 600 data) vs. 0 (Ni/NiO phase boundary) vs. = +30.8 (from Alloy X750 AH data). The ECP_{os} = +30.8 biases these calculations by ~3.2X in H_2.

Export Control Restrictions

Access to and use of EPRI Intellectual Property is granted with the specific understanding and requirement that responsibility for ensuring full compliance with all applicable U.S. and foreign export laws and regulations is being undertaken by you and your company. This includes an obligation to ensure that any individual receiving access hereunder who is not a U.S. citizen or permanent U.S. resident is permitted access under applicable U.S. and foreign export laws and regulations. In the event you are uncertain whether you or your company may lawfully obtain access to this EPRI Intellectual Property, you acknowledge that it is your obligation to consult with your company's legal counsel to determine whether this access is lawful. Although EPRI may make available on a case-by-case basis an informal assessment of the applicable U.S. export classification for specific EPRI Intellectual Property, you and your company acknowledge that this assessment is solely for informational purposes and not for reliance purposes. You and your company acknowledge that it is still the obligation of you and your company to make your own assessment of the applicable U.S. export classification and ensure compliance accordingly. You and your company understand and acknowledge your obligations to make a prompt report to EPRI and the appropriate authorities regarding any access to or use of EPRI Intellectual Property hereunder that may be in violation of applicable U.S. or foreign export laws or regulations.

The Electric Power Research Institute (EPRI)

The Electric Power Research Institute (EPRI), with major locations in Palo Alto, California; Charlotte, North Carolina; and Knoxville, Tennessee, was established in 1973 as an independent, nonprofit center for public interest energy and environmental research. EPRI brings together members, participants, the Institute's scientists and engineers, and other leading experts to work collaboratively on solutions to the challenges of electric power. These solutions span nearly every area of electricity generation, delivery, and use, including health, safety, and environment. EPRI's members represent over 90% of the electricity generated in the United States. International participation represents nearly 15% of EPRI's total research, development, and demonstration program.

Together…Shaping the Future of Electricity

Printed on recycled paper in the United States of America

1015288

Electric Power Research Institute
3420 Hillview Avenue, Palo Alto, California 94304-1338 • PO Box 10412, Palo Alto, California 94303-0813 • USA
800.313.3774 • 650.855.2121 • askepri@epri.com • www.epri.com